

**Distribution Agreement**

In presenting this thesis as a partial fulfillment of the requirements for a degree from Emory University, I hereby grant to Emory University and its agents the non-exclusive license to archive, make accessible, and display my thesis in whole or in part in all forms of media, now or hereafter now, including display on the World Wide Web. I understand that I may select some access restrictions as part of the online submission of this thesis. I retain all ownership rights to the copyright of the thesis. I also retain the right to use in future works (such as articles or books) all or part of this thesis.

Anoushka Mukhopadhyay

12.11.2024

Role of Mab21l2 Expression in the Development and Specification of Neurons in the Enteric  
Nervous System

by

Anoushka Mukhopadhyay

Iain Shepherd  
Adviser

Neuroscience and Behavioral Biology

Iain Shepherd  
Adviser

Andreas Fritz  
Committee Member

Leah Roesch  
Committee Member

2024

Role of Mab21l2 expression in the development and specification of neurons in the Enteric  
Nervous System

By

Anoushka Mukhopadhyay

Iain Shepherd  
Adviser

An abstract of  
a thesis submitted to the Faculty of Emory College of Arts and Sciences  
of Emory University in partial fulfillment  
of the requirements of the degree of  
Bachelor of Science with Honors

Neuroscience and Behavioral Biology

2024

## Abstract

### Role of Mab21l2 expression in the development and specification of neurons in the Enteric Nervous System

By Anoushka Mukhopadhyay

The enteric nervous system (ENS) is the largest subdivision of the peripheral nervous system. The ENS innervates the gut and regulates its function, though the mechanisms behind these processes are still not fully understood. ENS cells are derived from neural crest cells, and abnormal migration and specification of these cells manifest in pathologies of the ENS like Hirschsprung's disease (HSCR). Recently, single-cell-RNA sequencing studies in larval zebrafish have identified several previously uncharacterized cell populations, and regional specialization of the intestinal nervous system. Through a study of a multigenerational family with HSCR, a putative splice variant in the LRBA gene was identified within the linkage region previously associated with HSCR was identified. MAB21L2 is a gene embedded within the LRBA gene. This project investigated the role of *mab21l2* in enteric neuronal development and specification during early stages of gut development in zebrafish.

To accomplish this goal, we generated a *tg(phox2bb:egfp);mab21l2<sup>au12</sup>* mutant zebrafish line, done by crossing a *mab21l2<sup>au12</sup>* mutation onto a *tg:(phox2bb:egfp)* background. First generation larva were collected and fixed at 5 days post fertilization and then immunohistochemical stained with one of three different combinations of antibodies. The antibodies were anti-GFP used to label *phox2bb*<sup>+</sup> enteric cells, anti-5HT used to target serotonin producing cells, anti-HuC/D used to label all differentiated neurons in the gut (including those which are *phox2bb*<sup>-</sup>) and finally anti-nnos used to label inhibitory motor neurons. The larva were then blindly genotyped and guts dissected for confocal microscopic imaging. Images were processed to quantify the number of immune positively stained cells for each antibody.

*mab21l2* homozygous mutants displayed a significantly lower number of total *phox2bb*<sup>+</sup> enteric cells than their heterozygous and wildtype counterparts, suggesting that *mab21l2* expression affects the total all *phox2bb*<sup>+</sup> enteric cells. Moreover, Furthermore, *mab21l2* homozygous mutants showed significantly lower percentage of nos1<sup>+</sup> (nnos<sup>+</sup>) inhibitory motor neurons and *phox2bb*<sup>-</sup> HuC/D<sup>+</sup> enteric neurons. However, there was no significant difference on the percentage of serotonergic cells in *mab21l2* homozygous mutants relative to their heterozygote and wildtype counterparts. These results suggest that *mab21l2* potentially plays a role in the general development and specification of certain subtypes of neurons in the ENS subtypes. This study provides further novel insights into the cellular mechanisms that regulate enteric neuron development and differentiation.

Role of Mab21l2 expression in the development and specification of neurons in the Enteric  
Nervous System

By

Anoushka Mukhopadhyay

Iain Shepherd  
Adviser

A thesis submitted to the Faculty of Emory College of Arts and Sciences  
of Emory University in partial fulfillment  
of the requirements of the degree of  
Bachelor of Science with Honors

Neuroscience and Behavioral Biology

2024

## Acknowledgements

I would like to thank Dr. Iain Shepherd who conceived, designed, and guided the study. I would also like to thank my colleagues, Anna Han and Ana Tsulaia who aided with the data collection and analysis. Finally, I would like to thank Kaia Mukhopadhyay, Thea Mukhopadhyay and my parents for their support throughout my project.

## Table of Contents

Introduction .....	1
Figure 1 .....	2
Figure 2 .....	4
Figure 3 .....	7
Figure 4 .....	8
Figure 5 .....	12
Figure 6 .....	16
Materials and Methods .....	17
Table 1 .....	20
Figure 7 .....	22
Results .....	25
Figure 8 .....	25
Figure 9 .....	26
Figure 10 .....	29
Figure 11 .....	31
Figure 12 .....	32
Figure 13 .....	34
Figure 14 .....	36
Figure 15 .....	37
Figure 16 .....	39
Discussion .....	41
Conclusion .....	45
Bibliography.....	46

## Introduction

The enteric nervous system (ENS) is the largest subdivision of the peripheral nervous system. It functions autonomously, comprising of a neural network within the gastrointestinal tract. Its primary function is to coordinate essential physiological processes, such as the rhythmic contractions of peristalsis, nutrient absorption, secretion, and immune responses in the gut (Furness, 2012; Nezami & Srinivasan, 2010). The ENS achieves this through a well-coordinated network of sensory, motor, and interneurons that integrate local reflex circuits and establish bidirectional communication between the gut and the central nervous system (CNS) (Furness, 2006; Wood, 2008). The ENS can function independently of the CNS, a property that distinguishes it from other parts of the Peripheral Nervous System (PNS) and highlights its intrinsic complexity and functional autonomy, as demonstrated by its ability to maintain activity when studied in isolation *in vitro* (Grundy, 2006; Costa et al., 2000).

Anatomically, the ENS is organized into two principal plexuses: the myenteric plexus and the submucosal plexus, which are situated within distinct layers of the gut wall (Gershon & Tack, 2007). Within the gut wall, axons project from cell bodies to form interconnected networks innervating various structures, including muscle layers and the mucosa. The myenteric plexus lies between the longitudinal and circular muscle layers and is primarily responsible for regulating gut motility by coordinating contractions and relaxations of the intestinal muscles (Costa et al., 2000; Nurgali et al., 2007). Meanwhile, the submucosal plexus, located between the circular muscle layer and the mucosa, plays a crucial role in modulating glandular secretions, absorption, and blood flow by innervating enteroendocrine cells and epithelial tissues (Figure 1) (Brookes, 2001; Furness, 2006).

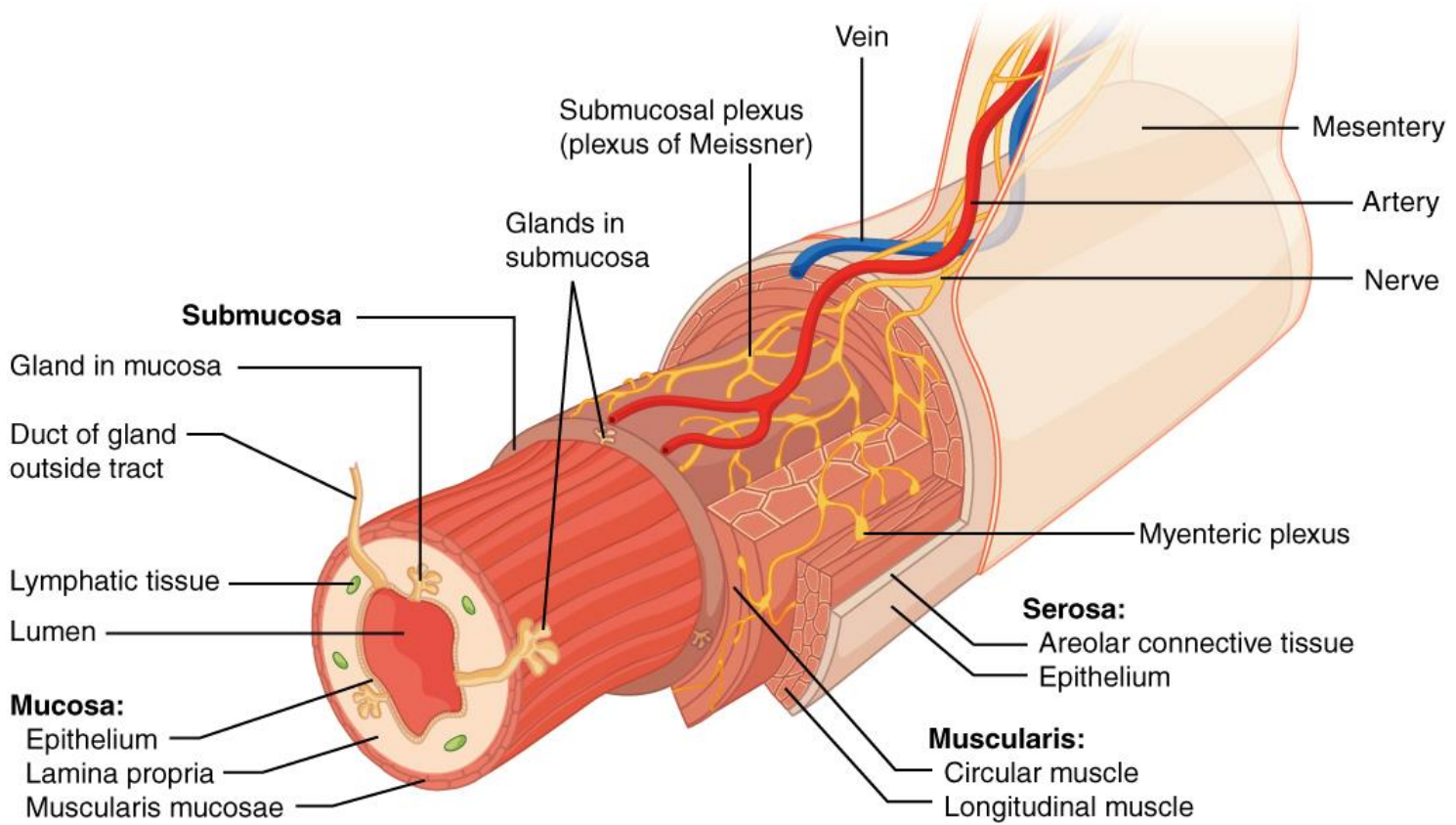


Figure 1. Cross-sectional view of the alimentary canal, illustrating its structural organization and components of the enteric nervous system (ENS).

The ENS features two primary plexuses: the myenteric plexus, located between the longitudinal and circular muscle layers, and the submucosal plexus, situated between the circular muscle layer and the mucosa. Key structures such as glands, lymphatic tissue, blood vessels, and the mesentery are also illustrated. (Connexions, OpenStax College, Anatomy & Physiology, Overview of the Digestive System).

## Functional Diversity of ENS Neurons

The ENS is characterized by a diversity of neuronal subtypes, which enables the precise regulation of gastrointestinal functions. In guinea pigs, 17 distinct types of neurons have been identified based on their morphology, neurotransmitter expression, and functional roles (Costa et al., 2000; Sang & Young, 1996). These neurons are broadly grouped into three main categories: intrinsic primary afferent neurons (IPANs), motor neurons, and interneurons. IPANs, which span both the myenteric and submucosal plexuses, are responsible for detecting mechanical changes in the gut wall and chemical properties of the luminal environment, serving as the sensory interface of the ENS (Kunze & Furness, 1999; Sang & Young, 1996). Motor neurons, localized in the myenteric ganglia, process input from interneurons and directly innervate the circular and longitudinal muscle layers to coordinate the rhythmic contractions and relaxations of peristalsis (Wood, 2008; Nurgali et al., 2007). Interneurons, which form integrative networks across multiple gut layers, relay signals between sensory and motor neurons, facilitating the communication necessary for complex reflex circuits (Grundy, 2006; Sang & Young, 1996). This organization forms the hierarchical nature of the ENS, with sensory neurons collecting environmental data, interneurons integrating signals, and motor neurons executing appropriate physiological responses (Gershon & Tack, 2007; Nezami & Srinivasan, 2010).

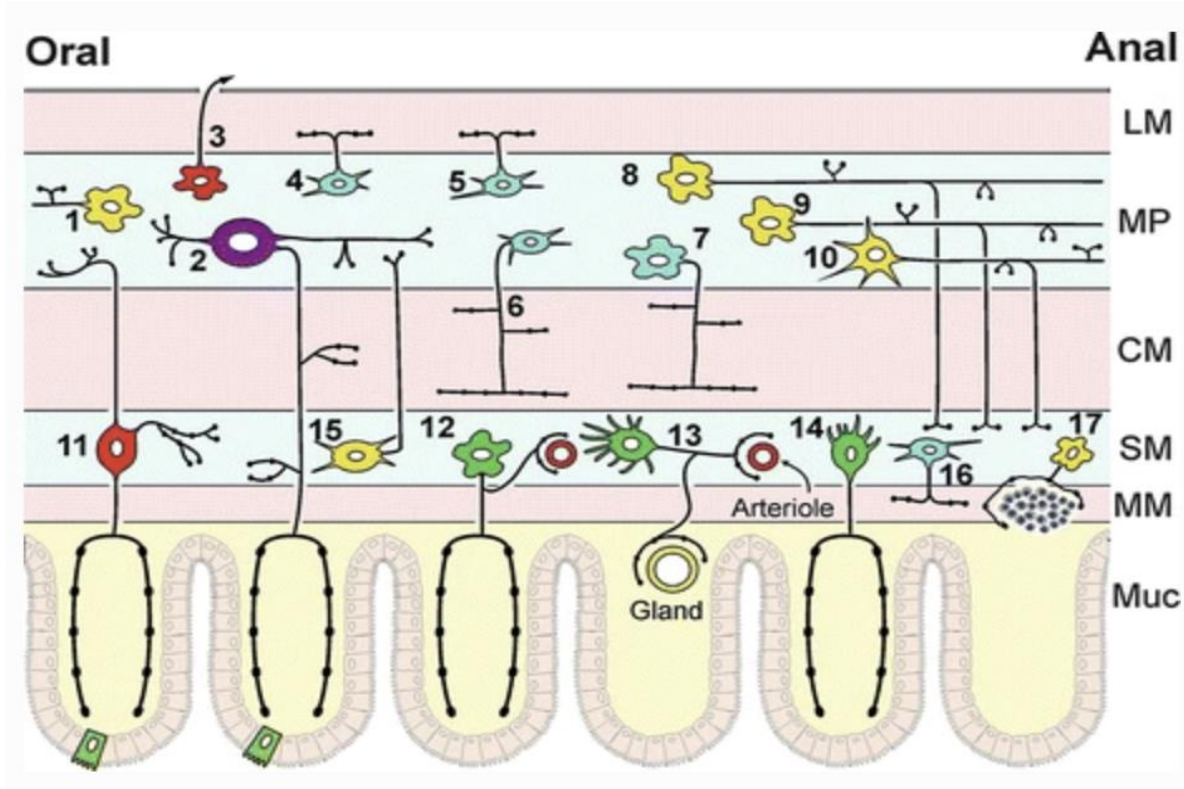


Figure 2 : Illustration of the 17 distinct neuron types within the enteric nervous system (ENS) of guinea pigs.

Categorized by roles and distribution across the gastrointestinal (GI) tract layers. The layers depict from top to bottom the longitudinal muscle (LM), myenteric plexus (MP), circular muscle (CM), submucosal plexus (SM), and mucosa (Muc). (Furness, John B., et al., 2014)

## **Model Systems**

The diversity and functionality of ENS neurons are not unique to guinea pigs but are conserved across species. Zebrafish are another organism that exhibit a comparable range of neuronal subtypes, including motor, sensory, and interneurons, that resemble those of higher vertebrates in function and neurochemical profile (Olsson et al., 2008; Holmberg et al., 2007). However, zebrafish lack certain anatomical features present in mammals, such as a submucosal plexus (Furness, 2006). Instead, their ENS comprises of a single, non-ganglionated myenteric plexus formed by individual neurons distributed along the gut wall (Shepherd & Eisen, 2011). Despite these differences, the zebrafish is a valuable model system for ENS research due to its rapid development, genetic tractability, and the complete formation of all major organ systems, including the ENS, by five days post-fertilization (5 dpf) (Kuil et al., 2020; Goldstein et al., 2017).

## **Relevance**

The ENS which is derived from neural crest cells, is a critical component of gastrointestinal function, forming a dense network of neurons and glial cells that regulate gut motility and homeostasis (Nagy & Goldstein, 2017; Burns & Thapar, 2006). During embryonic development, neural crest cells migrate from the neural tube along the length of the gastrointestinal tract to establish the ENS (Rao & Gershon, 2016; Wallace & Burns, 2005). Disruptions in this tightly orchestrated process can result in severe neuropathies, such as Hirschsprung disease (HSCR), a congenital disorder marked by the absence of enteric neurons in the distal bowel (Lake & Heuckeroth, 2013; Butler Tjaden & Trainor, 2013). This results in incapability of coordinating motility, leading to life-threatening complications like obstruction and inflammation (Amiel et al., 2008). While HSCR is one of the more thoroughly studied conditions, the molecular

mechanisms underlying the development and maintenance of the ENS—and other ENS-associated neuropathies—remain incompletely understood (Heanue & Pachnis, 2007).

### Transcriptomic Analyses

Single-cell RNA sequencing (scRNA-Seq) has provided significant insights into the developmental and functional complexity of the ENS. (Boesmans et al., 2015; Zeisel et al., 2018). The Shepherd Lab at Emory University, in collaboration with the Hofstra/Alves Lab at Erasmus University Rotterdam have undertaken an scRNA-Seq study of the development of the zebrafish ENS at five days post-fertilization (5 dpf) (Kuil, Laura E., et al., 2023). In this study 11 distinct neuronal clusters were identified, four of which represent differentiated enteric neuron subtypes (Kuil, Laura E., et al., 2023). (Figure 3) The largest cluster comprises of inhibitory motor neurons expressing the *nos1* gene, with a subset of serotonergic neurons characterized by *tph1* expression (Hao et al., 2016; Rao et al., 2021). Another major cluster, defined by the *nmu* gene, contains intrinsic primary afferent neurons (IPANs), while a third cluster represents motor neurons (Lasrado et al., 2017). The fourth cluster includes a diverse mix of glutamatergic, GABAergic, and additional IPAN subtypes (Boesmans et al., 2015). These findings align with similar transcriptomic studies in mice, where 21 neuronal clusters were classified into five functional groups: excitatory motor neurons, inhibitory motor neurons, sensory neurons, interneurons, and secretomotor/vasodilator neurons (Zeisel et al., 2018; Bellono et al., 2017). The identification of conserved genetic markers, such as *nos1* and *nmu*, across species underscores the evolutionary conservation of ENS development (Rao & Gershon, 2016). These transcriptomic analyses not only highlight the complexity and specificity of ENS neuronal subtypes but also reveal critical pathways and markers involved in their differentiation, providing

a foundation for future research into normal ENS function and associated GI disorders (Burns & Thapar, 2006; Goldstein et al., 2017).

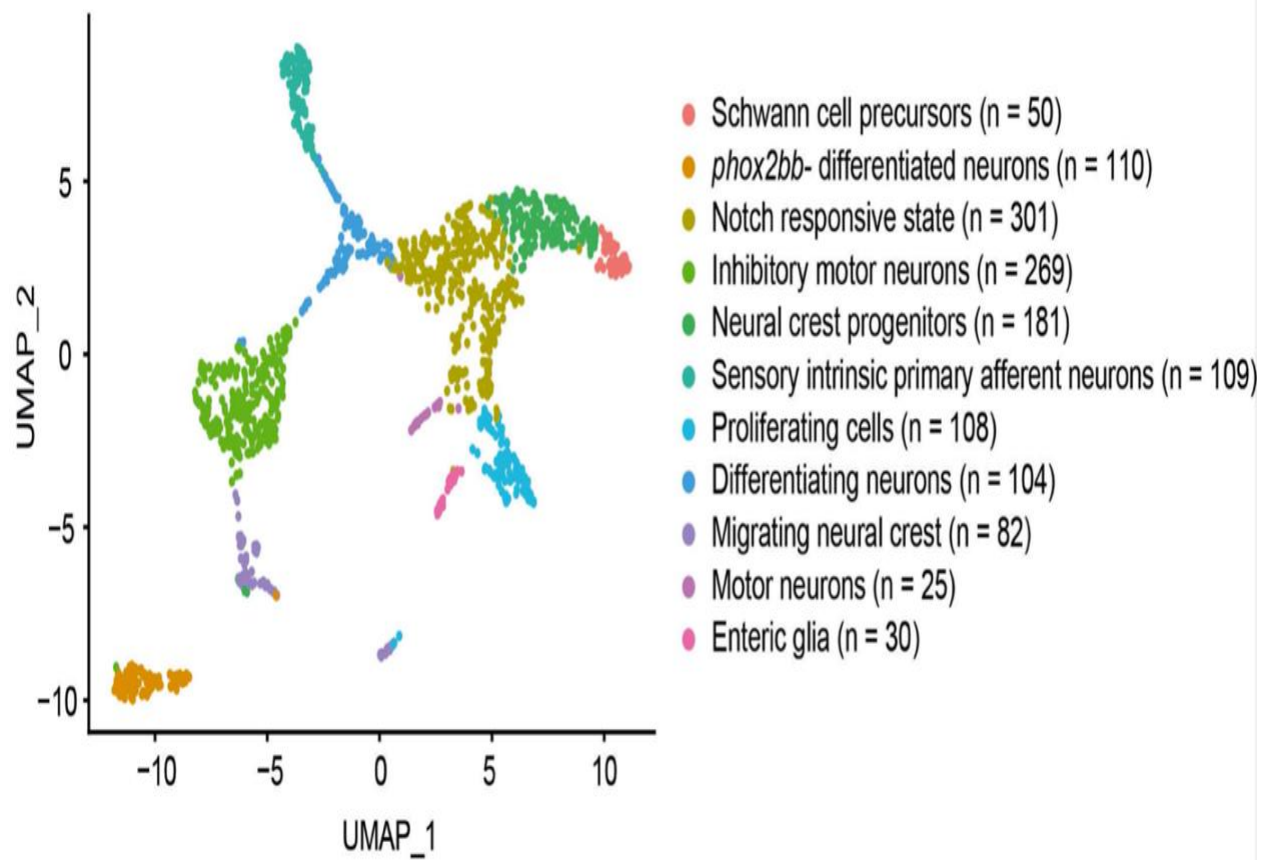


Figure 3: Transcriptomic Single Cell RNA sequencing data for the Zebrafish ENS at 5dpf.

A summary UMAP for the ENS generated from data from an scRNAseq analysis of 1369 ENS cells, showing eleven different clusters. (Kuil, Laura E., et al., 2023)

A pseudo-time trajectory analysis of ENS development in zebrafish reveals that neuronal precursors initially bifurcate into two major lineages: IPANs (branch 1) and inhibitory motor neurons (branch 2) (Shepherd & Eisen, 2011; Olsson et al., 2008). Further branching within the inhibitory motor neuron lineage gives rise to serotonergic neurons, amongst other differentiated and mature neurons, including *phox2bb*- cells. (Holmberg et al., 2007; Kuil et al., 2020) (Figure 4).

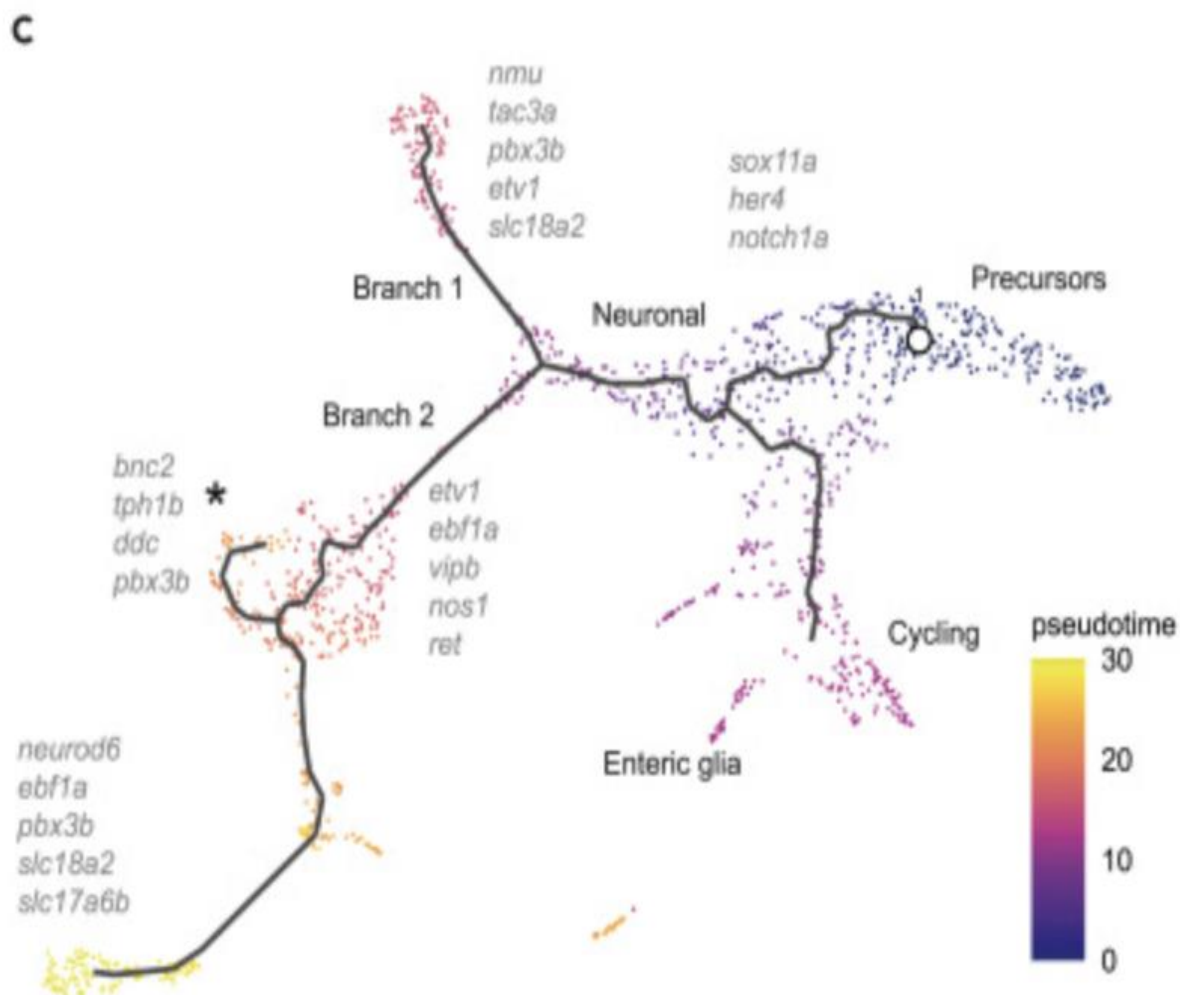


Figure 4: Color coded Pseudo time analysis showing a branching toward neuronal differentiation

## **MAB21L2**

The MAB21L2 gene (Mab-21-like 2) encodes a highly conserved protein that lies within intron 42 of the gene locus of *lrb1* in all vertebrate species and has emerged as a potential determinant in the development of the enteric nervous system (ENS) (Burns & Thapar, 2006; Zeisel et al., 2018). It is the vertebrate homologue of the gene male abnormal 21 first identified in *C. elegans* and has been shown via in vivo loss-of-function studies to have a role in development in multiple organ systems in multiple species (Nagy & Goldstein, 2017). Originally studied in vertebrates for its role in embryonic patterning, particularly in eye and craniofacial development, MAB21L2 more recently has gained attention for its contributions to the differentiation and specification of ENS neurons (Butler Tjaden & Trainor, 2013; Heanue & Pachnis, 2007). Recent studies utilizing single-cell RNA sequencing (scRNA-Seq) and other molecular techniques have highlighted its involvement in neural crest cell migration, neuronal subtype specification, and gastrointestinal function (Boesmans et al., 2015; Lasrado et al., 2017).

The following section explores the evidence supporting MAB21L2's role in ENS development, its expression patterns, and its clinical relevance in congenital GI disorders.

### **Transcriptomic Profiling**

Analysis of transcriptomic profiles has revealed that *mab21l2* is expressed in distinct neuronal subtypes within the ENS (Zeisel et al., 2018; Rao et al., 2021). In zebrafish, scRNA-Seq studies at five days post-fertilization (5 dpf) demonstrated robust *mab21l2* expression in neural crest-derived progenitors and differentiating motor and sensory neurons (Shepherd & Eisen, 2011; Goldstein et al., 2017). Notably, *mab21l2* was observed in intrinsic primary afferent neurons (IPANs) and subsets of inhibitory motor neurons, paralleling findings from mammalian models (Hao et al., 2016; Kuil et al., 2020). However, it showed limited expression in serotonergic

neurons, which instead prominently express the *tph1* gene encoding tryptophan hydroxylase (TPH), a key enzyme in serotonin biosynthesis (Holmberg et al., 2007; Rao et al., 2021). These findings underscore a potential lineage-specification role for *MAB21L2* during neuronal differentiation (Burns & Thapar, 2006; Boesmans et al., 2015).

In mammalian studies, including those in mice and humans, *MAB21L2* has shown evolutionary conservation in its expression patterns (Heanue & Pachnis, 2007; Wallace & Burns, 2005). scRNA-Seq analyses of mouse myenteric plexus neurons revealed that *MAB21L2* expression is enriched in inhibitory motor neurons and sensory subtypes, consistent with its role in zebrafish ENS development (Zeisel et al., 2018; Lasrado et al., 2017). Such conservation across species highlights its fundamental role in the differentiation of specific ENS subtypes and provides a valuable framework for studying ENS development in both model organisms and humans (Rao & Gershon, 2016; Shepherd & Eisen, 2011).

### **Molecular Mechanisms and Regulatory Role**

*MAB21L2* functions as a transcriptional regulator, likely binding to enhancer elements of genes essential for neuronal differentiation and function (Heanue & Pachnis, 2007; Boesmans et al., 2015). Transcriptomic profiling has shown that *MAB21L2* regulates the expression of critical developmental genes, including *PHOX2B*, *RET*, and *SOX10*, which are well-established regulators of ENS development (Butler Tjaden & Trainor, 2013; Goldstein et al., 2017). This places *MAB21L2* within the broader genetic network that governs neural crest migration, proliferation, and potentially differentiation (Lasrado et al., 2017; Zeisel et al., 2018). Its interaction with the BMP4-SMAD pathway further suggests a role in integrating extracellular signals with intracellular transcriptional responses, coordinating the specification of inhibitory motor and sensory neurons (Nagy & Goldstein, 2017; Burns & Thapar, 2006). Disruptions to

MAB21L2 expression in later life could potentially contribute to motility disorders or other ENS-related pathologies, such as irritable bowel syndrome (IBS) or chronic intestinal pseudo-obstruction (CIPO) (Lake & Heuckeroth, 2013; Rao & Gershon, 2016). Investigating its role in adult ENS maintenance and repair could reveal additional therapeutic targets (Hao et al., 2016; Shepherd & Eisen, 2011).

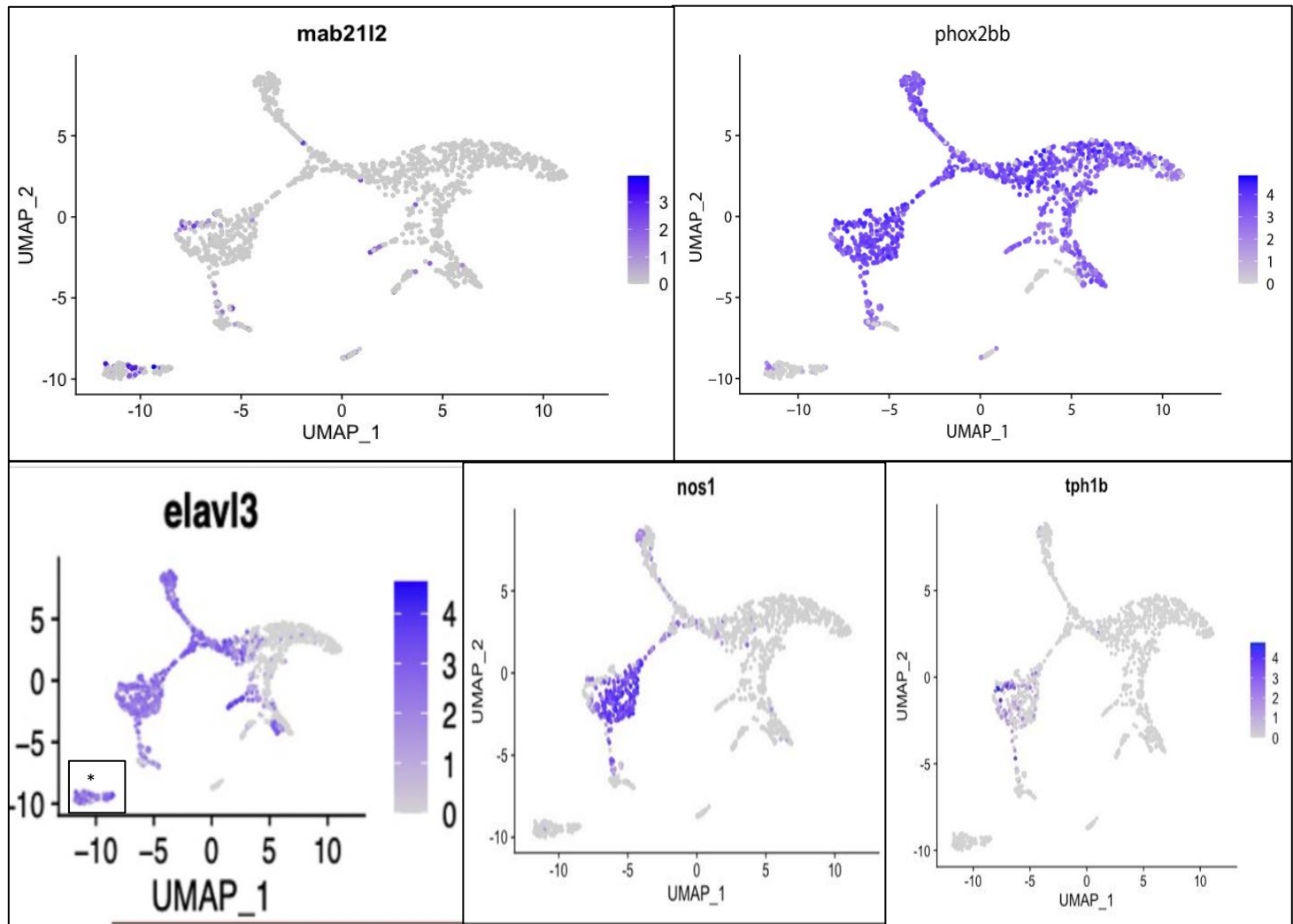


Figure 5: UMAPs showing the expression of *mab21l2*, *phox2bb*+, *elavl3*, *tph1b*, and *nos1* in the zebrafish ENS at 5dpf.

The gene expression patterns are visualizations that allow us to contextualize *mab21l2* expression relative to markers of general and subtype-specific neuronal populations.

The UMAP data highlights that *mab21l2* expression partially overlaps with *phox2bb*+ clusters, indicating that *mab21l2* may act in conjunction with or upstream of *phox2bb* during enteric neuron differentiation. This overlap supports the hypothesis that *mab21l2* contributes to the specification or maintenance of *phox2bb*+ cells, which are essential for ENS functionality. The co-localization of *mab21l2* and *elavl3* in UMAP space suggests that *mab21l2* may have a role in general neuronal differentiation. The overlap in expression occurs within specific clusters, suggesting that *mab21l2* is expressed in cells that are transitioning into mature neuronal states. The UMAPs for *mab21l2* and *tph1b* demonstrate a clear overlap, suggesting *mab21l2* may be important in the specification of serotonergic neurons. In contrast to serotonergic neurons, the UMAPs for *mab21l2* and *nos1* show more limited overlap, suggesting a less direct role in the differentiation of inhibitory motor neurons.

Based on these observations, the patterns of *mab21l2* expression in zebrafish 5dpf ENS UMAPs leads to our hypothesis that *mab21l2* is a potential regulator of neuronal subtype specification and differentiation in the zebrafish ENS. Its partial overlap with *elavl3*, *nos1* and *phox2bb* and specific overlap with *tph1b* neurons suggest that *mab21l2* may act both broadly in neuronal differentiation and more selectively in the specification of serotonergic and excitatory subtypes.

### **Functional Role in ENS Development and Specification**

Functional studies have previously implicated MAB21L2 as a key determinant of ENS neuronal differentiation (Heanue & Pachnis, 2007; Lasrado et al., 2017). Like other transcriptional regulators, MAB21L2 interacts with signaling pathways essential for neural crest cell development, particularly the BMP4-SMAD axis (Butler Tjaden & Trainor, 2013; Nagy & Goldstein, 2017). BMP4 signaling is known to influence neural crest cell differentiation and neuronal fate (Goldstein et al., 2017; Burns & Thapar, 2006). MAB21L2's interaction with

SMAD1 suggests that it could co-regulate transcriptional programs governing the specification of IPANs, inhibitory motor neurons, and other ENS subtypes (Boesmans et al., 2015; Hao et al., 2016). Previous loss-of-function studies in zebrafish have demonstrated that a *mab21l2* mutation results in significant disruptions to ENS development, including reduced neuronal counts and a failure to fully populate the distal gut with enteric neurons (Kuil et al., 2020; Shepherd & Eisen, 2011). These defects are reminiscent of human conditions like Hirschsprung disease (HSCR), where neural crest migration and differentiation are disrupted (Amiel et al., 2008; Lake & Heuckeroth, 2013).

We believe a detailed experimental study could further delineate *mab21l2*'s function by comparing neuronal numbers and subtypes across wild-type, heterozygous, and homozygous mutant zebrafish embryos. This approach would help clarify its role in subtype specification, particularly for serotonergic neurons, IPANs, and inhibitory motor neurons.

### **Expression Patterns and Developmental Timing**

Previous studies by the Shepherd lab have shown that *mab21l2* expression has a distinct pattern of gene expression during ENS development (Shepherd & Eisen, 2011; Kuil et al., 2020). In zebrafish, it is detected as early as 48 hours post-fertilization (hpf), during the migration of neural crest cells along the gut (Goldstein et al., 2017; Burns & Thapar, 2006). By 72 hpf, *mab21l2* expression is concentrated in the developing myenteric plexus, coinciding with the differentiation of motor and sensory neurons (Nagy & Goldstein, 2017; Boesmans et al., 2015). This temporal and spatial pattern of expression supports its role in potentially driving the transition from neural crest progenitors to differentiated ENS neuronal subtypes (Lasrado et al., 2017; Zeisel et al., 2018).

In situ hybridization studies in zebrafish embryos have revealed an expression pattern along the gut, persisting through 120 hpf, aligning with the critical stages of ENS formation (Hao et al., 2016; Holmberg et al., 2007). In previous research, morpholino knockdown of *mab21l2* resulted in a reduction in ENS neuronal number (Butler Tjaden & Trainor, 2013; Shepherd & Eisen, 2011). In situ gene expression analysis using an antisense digoxigenin-labeled RNA probe showed that the *mab21l2* gene is expressed in the gut during the early stages of ENS development (Goldstein et al., 2017; Burns & Thapar, 2006). Figure 6 shows the expression pattern of *mab21l2* from 24 hpf to 96 hpf. *mab21l2* is expressed along the length of the gut from 48 hpf. This data supports the idea that *mab21l2* is present at the right time in the right place to potentially play a role in ENS development in zebrafish (Lasrado et al., 2017; Kuil et al., 2020).



Figure 6: Expression of mab21l2 in the zebrafish gut during early ENS development. In situ hybridization using an antisense digoxigenin-labeled RNA probe demonstrates mab21l2 expression from 24 to 96 hours post-fertilization (hpf). Significant expression along the length of the gut is observed starting at 48 hpf, coinciding with critical stages of ENS development.

Due to the significant expression of *mab21l2* gene in specific differentiated neuronal clusters as well as the observed in vivo pattern of *mab21l2* RNA expression, we hypothesized that *mab21l2* gene may play a role in the development and differentiation of specific ENS neuronal subtypes in zebrafish. We intend to test this hypothesis by undertaking a detailed quantitative examination of ENS subtypes in genotyped 5dpf embryos derived from an in cross of *mab21l2 heterozygous* mutant zebrafish. By quantifying and comparing the total number of enteric neurons and the respective proportions of serotonergic neurons, *phox2bb*-negative neurons, and inhibitory motor neurons across in these genotyped embryos we seek to elucidate the role of *mab21l2* in shaping ENS neuron subtype diversity in zebrafish.

## Materials and methods

### **Zebrafish Line Maintenance and Breeding**

The *mab21l2<sup>au12</sup>* zebrafish mutant line was sourced from the Zebrafish International Resource Center (ZIRC) and crossed with the transgenic *tg:(phox2bb:egfp)* strain. This mutation results from a single nucleotide substitution (A to T) at nucleotide 301, introducing a premature stop codon. The *phox2bb:egfp* transgenic line was generated using a background containing the *phox2bb* locus, which was engineered to incorporate the enhanced green fluorescent protein (*egfp*) at its native start site. This modification was introduced through a bacterial artificial chromosome (BAC) and subsequently used to establish the transgenic line (Raible *et al.*, 2008). This modification allows for GFP expression driven by the *phox2bb* promoter, facilitating the visualization of enteric neurons expressing this gene (Burns & Thapar, 2006; Kuil *et al.*, 2020; Goldstein *et al.*, 2013).

For this study, GFP+ embryos were obtained by crossing homozygous *tg:(phox2bb:egfp)*

individuals with heterozygous fish carrying the *mab2112<sup>au12</sup>* allele. Adult zebrafish with the *tg:(phox2bb:egfp); mab2112<sup>au12</sup>* genotype were genotyped using DNA extracted from fin clips. Based on their *mab2112<sup>au12</sup>* genotype, the zebrafish were grouped into three distinct categories—wild-type (+/+), heterozygous (+/-), and homozygous mutant (-/-)—and maintained in separate tanks. To generate embryos for analysis of enteric nervous system (ENS) neuronal differentiation and specification, three females and two males of each genotype were set up in a breeding tank overnight.

### **Immunohistochemistry Protocol**

Embryos from an in-cross of *tg:(phox2bb:egfp)<sup>+/+</sup>; mab2112<sup>au12+/-</sup>* fish were collected at 5 days post-fertilization (5 dpf) for double-labeling immunohistochemistry. Embryos were first fixed in a solution of 4% paraformaldehyde prepared in 1X fix buffer for two hours, followed by three 10-minute washes in PBS containing 0.5% Triton X-100 (PBT). Subsequently, they were rinsed three times in distilled water over a one-hour period. To block non-specific antibody binding, embryos were incubated for one hour in a blocking solution containing 5% goat serum. The embryos were then incubated overnight with primary antibodies diluted in the blocking solution. Afterward, they were washed three times for 30 minutes each with PBT and then incubated with the appropriate secondary antibodies diluted in blocking solution for 16–18 hours. Following another series of washes with PBT, the embryos were stored in PBT containing 0.01% sodium azide.

The primary and secondary antibodies used in the staining procedures were as follows:

1. For 5-HT Staining:

A rabbit polyclonal antibody targeting serotonin (5-HT), coupled with bovine serum

albumin and paraformaldehyde (Immunostar), was used at a 1:10,000 dilution. This was paired with a mouse monoclonal primary antibody specific to GFP (Invitrogen) for detecting *phox2bb*-driven GFP expression. Secondary antibodies included goat anti-mouse Alexa Fluor 488 and goat anti-rabbit Alexa Fluor 594 (Invitrogen).

2. For HuC/D Staining:

A mouse monoclonal antibody targeting the HuC/D protein which encoded by *elavl3* (a human neuronal protein D-derived synthetic peptide; Invitrogen) was used at a 1:50 dilution, paired with a rabbit polyclonal anti-GFP antibody. Secondary antibodies used were goat anti-mouse Alexa Fluor 568 and goat anti-rabbit Alexa Fluor 488 (Invitrogen).

3. For nNos Staining:

A rabbit polyclonal antibody targeting nNos, the protein product of the *nos1* gene, (a synthetic human nNos peptide; Abcam) was used, paired with a mouse monoclonal primary antibody specific for GFP (Invitrogen) for detecting *phox2bb*-driven GFP expression. Secondary antibodies included goat anti-mouse Alexa Fluor 488 and goat anti-rabbit Alexa Fluor 594 (Invitrogen).

### **Genotyping of Stained 5 dpf Embryos**

To determine the genotypes of the 5 days post-fertilization (5 dpf) embryos following immunohistochemical staining, DNA extraction was performed after dissection using the Invitrogen Platinum Direct PCR kit. The heads of the stained embryos were carefully removed to isolate DNA while preserving tissue integrity. DNA was extracted using a lysis protocol optimized for zebrafish samples. For amplification of the *mab21l2* gene, a polymerase chain reaction (PCR) using the Invitrogen Platinum Direct PCR kit was performed using primers specific to *mab21l2*: (Table 1).

The PCR setting were standard with an annealing temperature of 55°C to promote efficient primer binding. A total of 49 amplification cycles were conducted to generate sufficient quantities of the target DNA. Once amplified, the PCR product was purified using the QIAquick PCR purification kit, to ensure high-quality DNA sample suitable for downstream sequencing. The purified DNA was then submitted to Psomagen for sequencing to confirm the nucleotide sequence of the amplified region. Sequencing data was analyzed using Sequencher software, enabling accurate alignment and identification of sequence variations. This analysis confirmed the genotypes of the stained embryos, differentiating wild-type, heterozygous, and homozygous individuals based on the presence or absence of the *mab21l2<sup>au12</sup>* mutation.

Table 1: Sequences of the Exon 8 2Forward and Exon 8 2Reverse primers

Primer	Sequence
Forward	5' - CGA GAG GTG TGT AAG GTG GT -3'
Reverse	5' - GCA TTT CTT CCT ACA GCC CG -3'

### **Imaging and Analysis**

The guts of genotyped embryos were dissected and imaged using an Olympus Spinning Disk Confocal Microscope, operated in conjunction with SlideBook 6 x64 software. Initially, imaging was performed at 20x magnification, but the procedure was amended midway to use 10x magnification. This adjustment allowed for capturing the entire gut tube in a single frame, providing a more comprehensive view of the gut's neuronal composition and reducing variability caused by partial imaging of the tissue.

During imaging, the gut tube was positioned horizontally within the frame to ensure consistent orientation across samples. The mid/posterior region of the gut was specifically targeted for imaging under both green (GFP) and red (RFP) fluorescence channels. *phox2bb*<sup>+</sup> neurons, which were labeled by secondary antibodies conjugated with Alexa Fluor<sup>TM</sup> 488 to recognize GFP, fluoresced green. Neurons expressing anti-5HT, anti-HuC/D and anti-nNOS antibodies fluoresced red due to secondary antibodies conjugated with Alexa Fluor<sup>TM</sup> 568, 647 and 594, respectively. Confocally projected images were captured for each gut, and these images were saved and exported as 24-bit TIF files for analysis.

### **Quantitative Analysis**

TIF files were processed in Adobe Photoshop to convert fluorescence images into black-and-white formats, ensuring clarity for cell counting. These black-and-white images were subsequently analyzed using ImageJ, software that can be used to quantify the number of neurons by pixel color (figure 7). This allowed for standardization and minimization of human error.

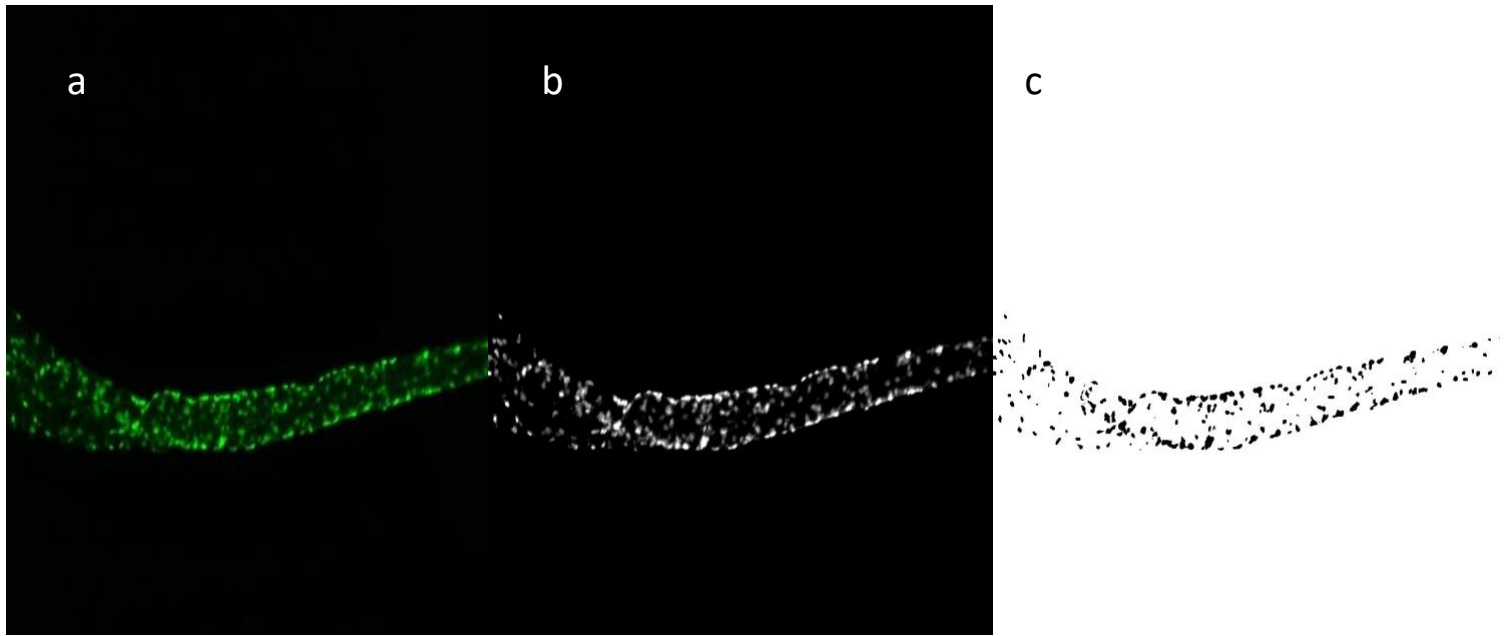


Figure 7: Image processing. Images collected from the confocal microscope (a) were first adjusted in Adobe photoshop (b), and then in ImageJ (c) before the latter was used to quantify neuronal counts.

Counts were conducted for all neurons captured in the frame and four sets of data were collected:

1. Total number of neurons (*phox2bb*<sup>+</sup> neurons).
2. Total number and proportion of serotonergic neurons (5HT<sup>+</sup> and *phox2bb*<sup>+</sup> neurons).
3. Total number and proportion *phox2bb*<sup>-</sup> neurons (HuC/D<sup>+</sup> and *phox2bb*<sup>+</sup> neurons)
4. Total number and proportion of inhibitory motor neurons (nos1<sup>+</sup> and *phox2bb*<sup>+</sup> neurons).

The proportions of each neuronal subtype relative to the total number of neurons were calculated for each sample. Data were then organized and plotted in Excel using a stacked dot plot format. These plots displayed three distinct groups: wild-type (+/+), heterozygous (+/-), and mutant (-/-) embryos. Each dot represented an individual embryo, with its position indicating the count or percentage, and average of a specific neuronal subtype on the y axis and its allelic identity on the x axis.

### **Statistical Analysis**

To evaluate the significance of differences between groups, a paired T-test with equal variance and a p-value threshold of 0.001 was applied. Statistical comparisons included the total number of neurons and the proportions of serotonergic, *phox2bb*<sup>-</sup>, and inhibitory motor neurons between groups. Significant differences were marked with an asterisk (\*) or (\*\*), while non-significant results were labeled as "n.s." (not significant).

The switch to 10x magnification improved the reliability of these analyses by ensuring the entire gut was imaged, capturing all neuronal subtypes in their proper anatomical context. This adjustment minimized bias and provided a more accurate reflection of the neuronal composition within each group.

Since data were collected using two different magnifications (10x and 20x), the potential differences in imaging coverage and field of view were accounted for in the graphical analysis.

Scaling was applied to one of the graphs to ensure that data from both magnifications were directly comparable. This scaling process adjusted the numerical values to reflect the same proportional coverage of the gut across all samples, enabling consistent and accurate visualization of the results regardless of the imaging magnification used.

## Results

### *phox2bb*<sup>+</sup> and Serotonergic (5HT<sup>+</sup>) Cell Counts

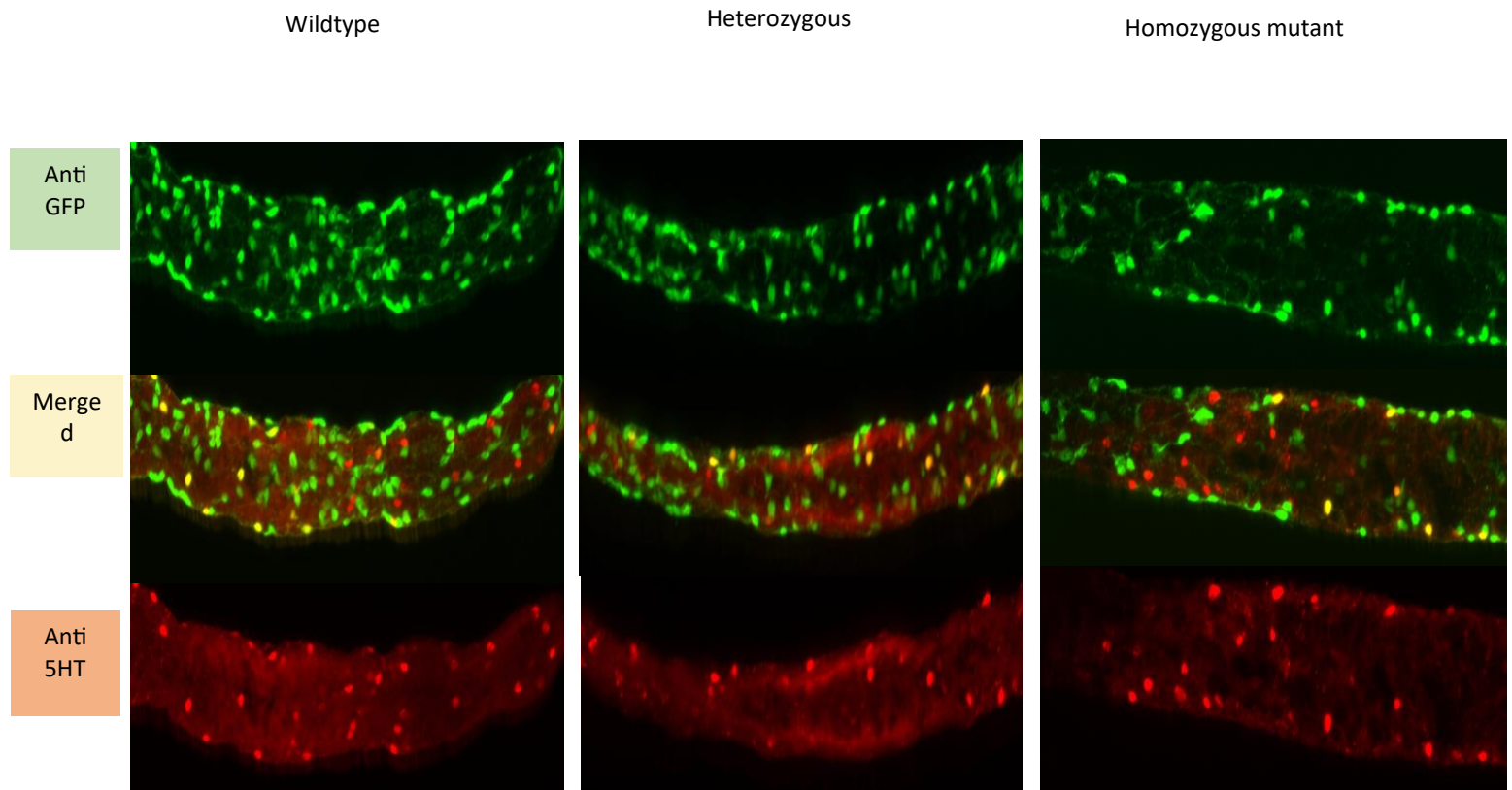


Figure 8: confocal images of wildtype, heterozygous, and homozygous mutant zebrafish guts at 5dpf embryos stained with Anti-GFP and Anti-5HT markers. The guts of *mab21l2* homozygous mutant embryos show a decrease in the number of *phox2bb*<sup>+</sup> cells. There is no significant difference in the number of 5HT<sup>+</sup> cells across the genotypes.

**phox2bb positive cells are significantly reduced in anti-GFP and anti-5HT mab21l2 mutants, suggesting an integral role for mab21l2 in the general development neurons in the enteric nervous system.**

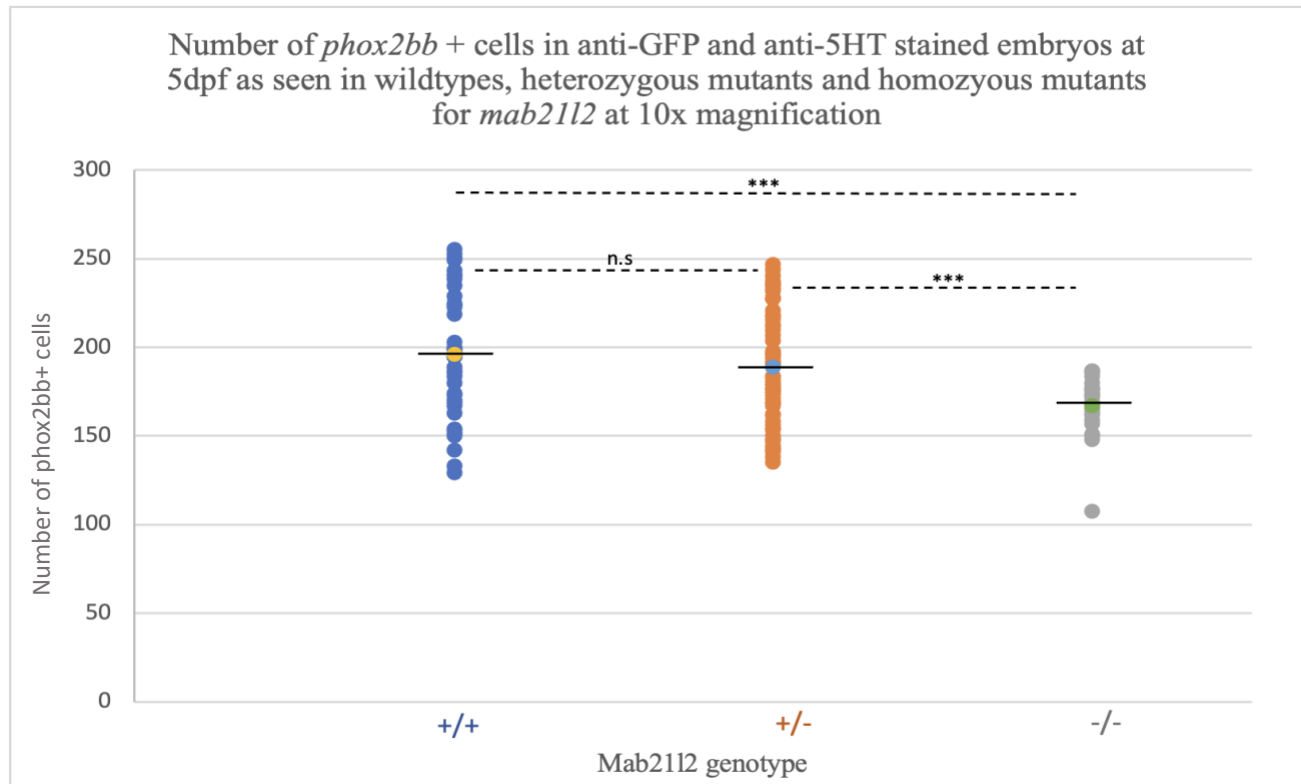


Figure 9: Total number of *phox2bb*+ neurons in 5dpf across wildtype, heterozygote, and homozygous mutant embryos for the *mab21l2* gene stained with anti-GFP and anti-5HT antibodies. No significant difference between the total number of neurons between wildtype and heterozygote mutant with threshold  $p>0.05$ . *Homozygous* mutants display a significantly lower number of *phox2bb*+ cells than heterozygote mutants and wildtypes with threshold  $p<0.001$ (denoted by \*\*\*)

*mab21l2* homozygous mutant embryos stained with anti-GFP and anti-5HT antibodies exhibited a significantly lower total number of *phox2bb*+ cells at 5 days post-fertilization (5 dpf) compared to heterozygous and wildtype embryos. A total of 42 wildtype, 67 heterozygous, and 27 homozygous mutant 5 dpf embryos were stained using anti-GFP and anti-5HT primary antibodies and complementary secondary antibodies (goat anti-mouse Alexa Fluor 488 and goat anti-rabbit Alexa Fluor 594). Representative gut images for all three genotypes are shown in Figure 8.

In these images, red fluorescence (dots) corresponds to cells producing serotonin, recognized by the anti-5HT antibody. Green fluorescence (dots) indicates nearly all enteric neurons and neural crest cell precursors expressing the *phox2bb* gene and producing green fluorescent protein (GFP), which is bound by the anti-GFP antibody. Axonal projections extending from these *phox2bb*+ enteric neurons appear as lines extending from green dots. *phox2bb* is broadly expressed in nearly all enteric neuronal subtypes and progenitors and absent in non-neuronal ENS cells (apart from undifferentiated neural crest cells). In contrast, red fluorescence marks all serotonin-producing cells, including both *phox2bb*+ serotonergic neurons and non-neuronal enteroendocrine cells that produce serotonin but do not express *phox2bb*.

In merged images, yellow fluorescence denotes serotonergic neurons which express both *phox2bb* and *tph1b* genes. These cells fluoresce green due to GFP produced under the control of the *phox2bb* gene and red due to serotonin being recognized by the anti 5HT primary antibody and is produced by the enzyme encoded by *tph1b*. Cells fluorescing exclusively red represent non-neuronal enteroendocrine cells, which express *tph1b* but lack *phox2bb* expression, and therefore do not bind anti-GFP antibodies.

During the course of this experiment, imaging magnification was adjusted from 20x to 10x to ensure that the entire gut tube could be captured within a single frame. This change improved consistency by providing a more comprehensive representation of the gut's neuronal composition. To account for differences arising from this shift, all quantitative data were scaled to reflect the 10x imaging field, ensuring that results from both magnifications were directly comparable.

From the gut images, it is evident that heterozygous embryos show a slight reduction in the overall count of *phox2bb*<sup>+</sup> cells compared to wildtypes. However, homozygous *mab21l2* mutants display a much more pronounced reduction in *phox2bb*<sup>+</sup> neurons relative to both heterozygotes and wildtypes. Statistical analysis revealed no significant difference in the total number of *phox2bb*<sup>+</sup> cells between heterozygotes and wildtypes ( $p = 0.8038$ ). However, homozygous mutants displayed a significant reduction in the total number of *phox2bb*<sup>+</sup> cells compared to both heterozygotes ( $p = 0.001$ ) and wildtypes ( $p = 0.0001$ ).

Furthermore, serotonergic neurons are also reduced in the gut of homozygous mutants, although the overall count of 5HT<sup>+</sup> cells, including non-neuronal enteroendocrine cells, showed no significant difference between wildtype, heterozygote, and mutant embryos.

To assess these differences, data on the serotonergic cells as a percentage of total number of *phox2bb*<sup>+</sup> cells, are shown plotted below.

**Serotonergic neurons show no significant reduction in *mab21l2* mutants, suggesting no instructive signaling provided by *mab21l2* for serotonergic specification.**

Percentage of serotonergic cells of total cells in anti-GFP and anti-5HT stained 5dpf embryos as seen in wildtypes, heterozygous mutants and homozygous mutants for *mab21l2* at 10x magnification

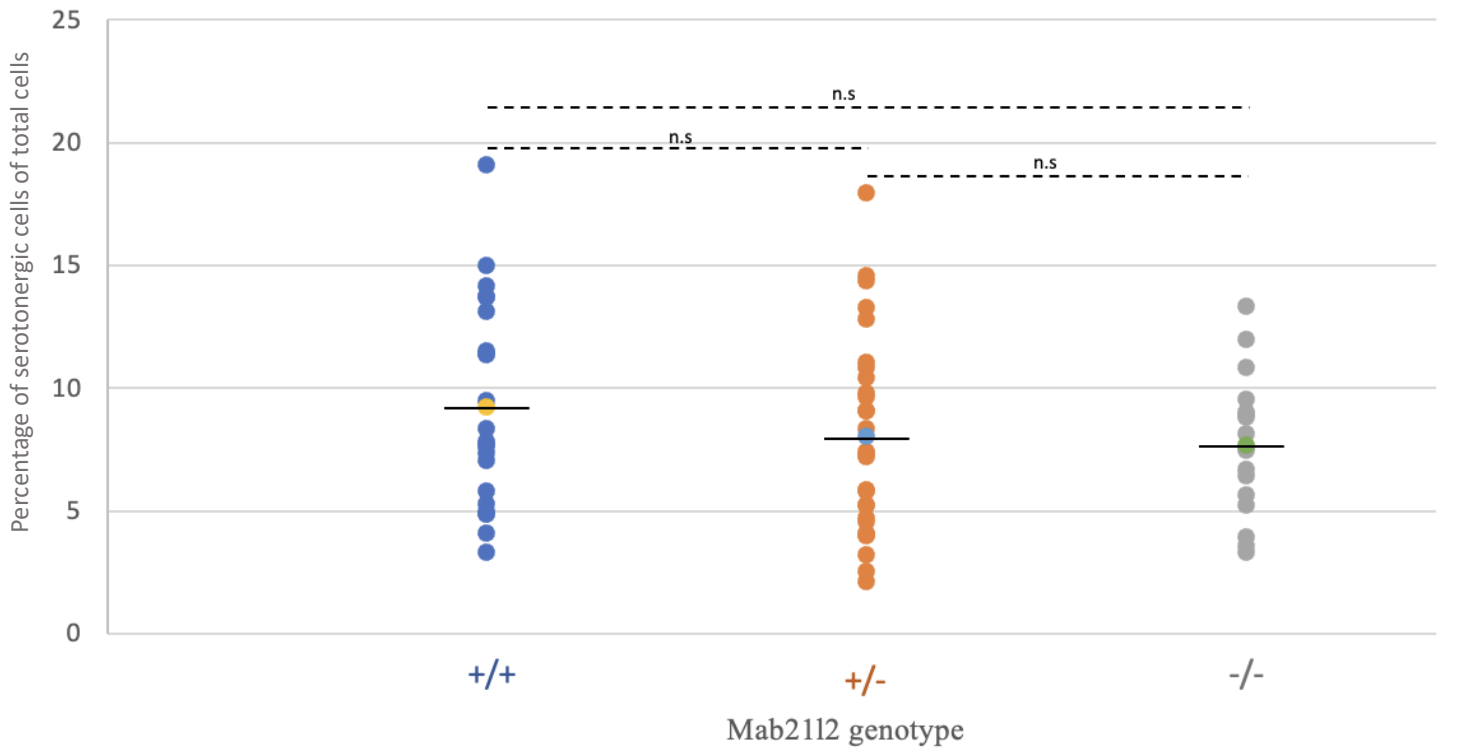


Figure 10: Percentage of serotonergic neurons as a percentage of total neurons across wildtype, heterozygote, and homozygous mutant embryos for the *mab21l2* gene stained with anti-GFP and anti-5HT antibodies. No significant difference observed with threshold p>0.05

When analyzing the total count of serotonergic neurons as a percentage of total neurons, no significant differences are observed across the three genotypes (Figure 10). Statistical analysis reveals no significant reduction in 5HT<sup>+</sup> cells between wildtype and homozygous mutants ( $p = 0.9590$ ), wildtype and heterozygotes ( $p = 0.1953$ ), or heterozygotes and homozygous mutants ( $p = 0.2625$ ). This indicates that the overall population of serotonergic neurons remains consistent across the genotypes.

Absolute counts of 5-HT<sup>+</sup> cells (that encompass both serotonergic and enteroendocrine cells) and serotonergic neurons, which co-express both the *phox2bb* and *tph1b* genes, no statistically significant reduction is observed between any of the genotypes. Although serotonergic neurons fluoresce as yellow due to overlapping green (GFP) and red (5HT) fluorescence, quantitative analysis shows that their numbers do not vary significantly among wildtypes, heterozygotes, and mutants. These results suggest that the mechanisms underlying serotonin production are not significantly disrupted by the loss of *Mab21l2*.

The consistency in 5HT<sup>+</sup> cell counts contrasts sharply with the significant reduction observed in the total number of *phox2bb*<sup>+</sup> cells in homozygous mutants. The lack of a significant decrease in serotonergic neurons compared to the significant reduction in *phox2bb*<sup>+</sup> neurons implies that serotonergic neurons are relatively preserved despite the overall decline in the broader enteric neuron population. This result suggests the potential role of *mab21l2* in influencing the general development of the enteric nervous system, rather than acting specifically on specifying the serotonergic enteric neuronal subtype. Its impact suggests that *mab21l2* broadly regulates neuronal population dynamics and overall ENS development. It may reflect compensatory mechanisms that prioritize the development or maintenance of serotonergic neurons, or it could

suggest that *mab21l2* plays a more critical role in the specification of other enteric neuronal subtypes.

#### ***phox2bb*+** Enteric Neuronal and ***phox2bb*-** enteric neuron Cell Counts

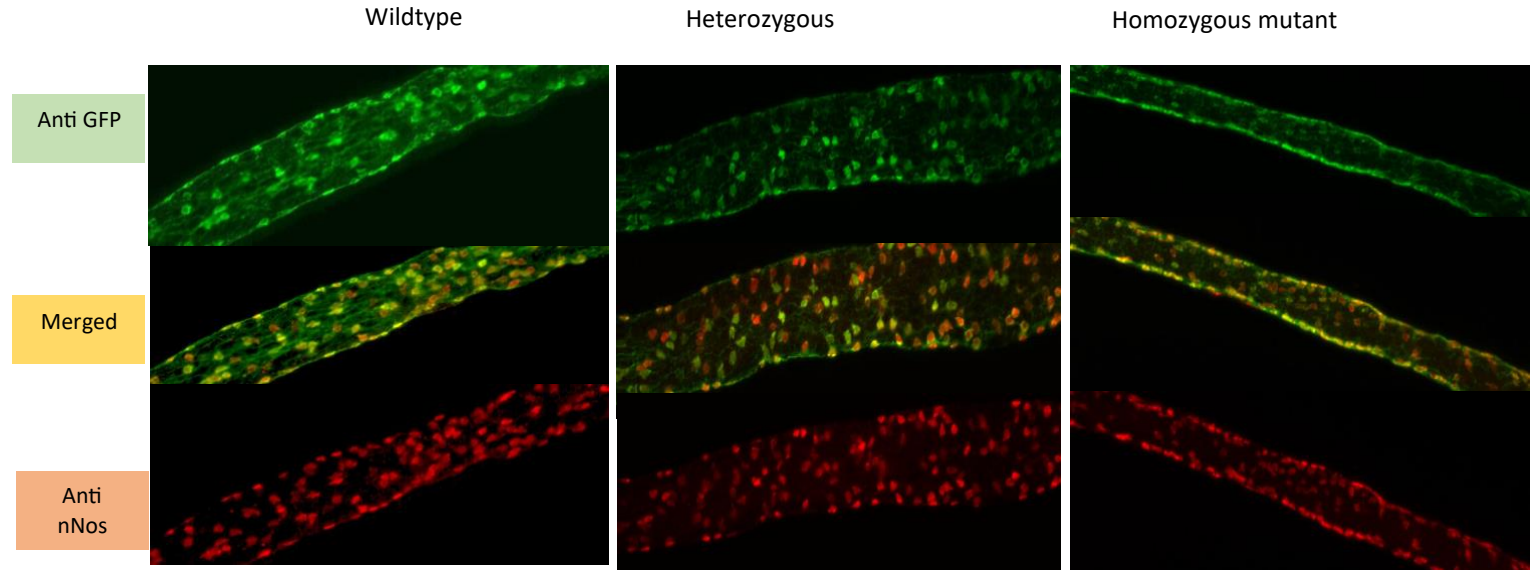


Figure 11: confocal images of wildtype, heterozygous, and homozygous mutant zebrafish guts at 5dpf embryos stained with Anti-GFP and Anti-HuC/D markers. The guts of *mab21l2* homozygous mutant embryos show a decrease in the number of *phox2bb*+ cells and a modestly significant decrease in percentage of *phox2bb*- cells.

*phox2bb* positive cells are significantly reduced in anti-GFP and anti-HuC/D stained *mab21l2* mutants, suggesting an integral role for *mab21l2* in the general development neurons in the enteric nervous system.

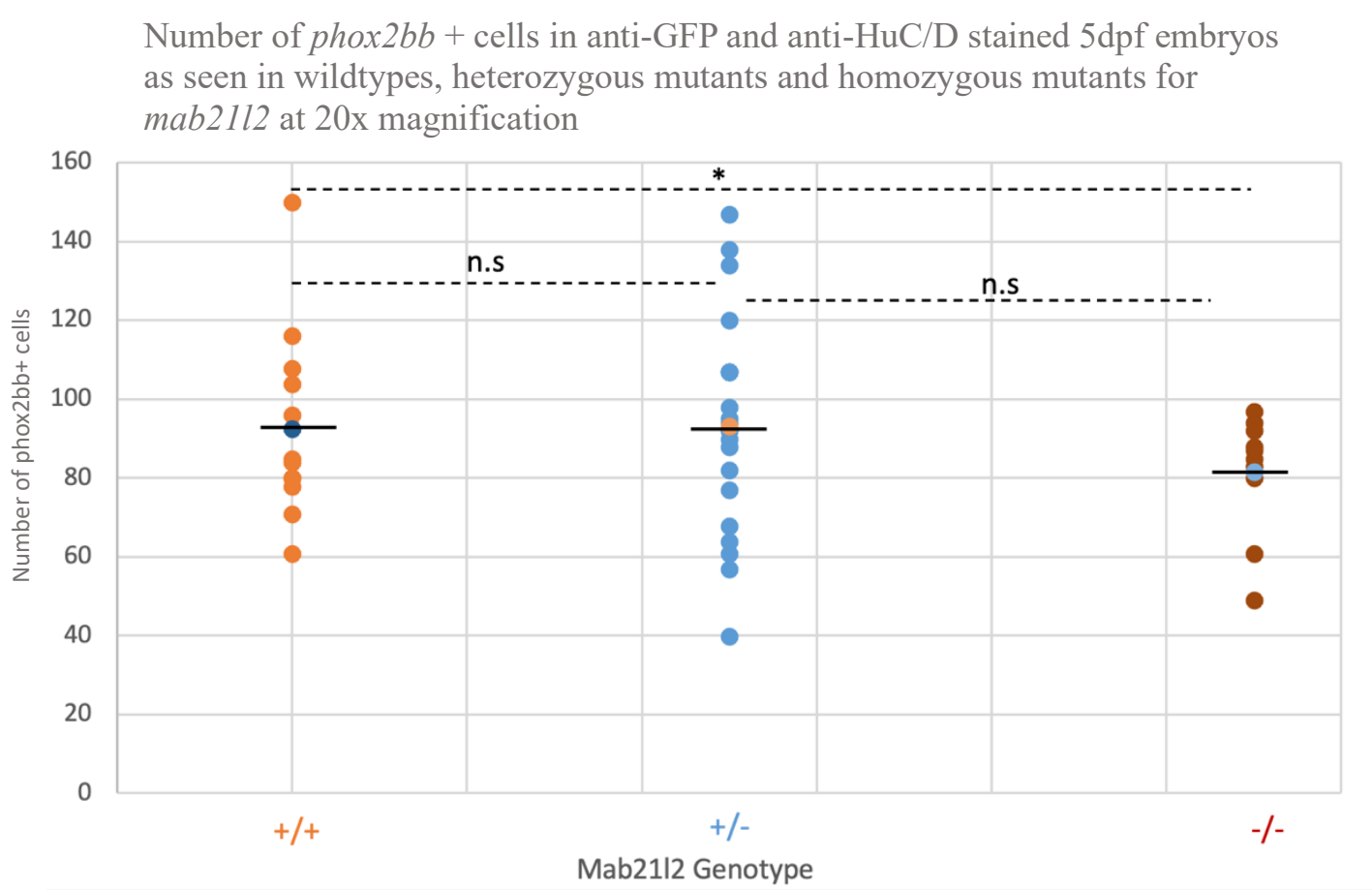


Figure 11: Total number of *phox2bb* + cells in 5dpf across wildtype, heterozygote, and homozygous mutant embryos for the *mab21l2* gene stained with anti-GFP and anti-HuC/D antibodies. No significant difference between the Wildtype and Heterozygote, and between mutant and heterozygote mutant with threshold  $p>0.05$ . Homozygous mutants display a significantly lower number of *phox2bb* + cells than wildtypes with threshold  $p<0.05$  (denoted by \*).

To assess the distribution of *phox2bb*<sup>+</sup> neurons, embryos from three genotypes—wildtype, heterozygous, and homozygous mutant—were stained with HuC/D antibodies and analyzed co expression with the GFP fluorescence. A total of 14 wildtype, 22 heterozygous, and 11 homozygous mutant embryos were examined. In the gut images, each red dot represents a HuC/D<sup>+</sup> neurons, while each green dot corresponds to a *phox2bb*<sup>+</sup> cells as revealed by anti-GFP and anti-HuC/D primary antibodies and complementary secondary antibodies (goat anti-mouse Alexa Fluor 488 and goat anti-rabbit Alexa Fluor 647). Representative gut images for all three genotypes are shown in Figure 10.

Notably, most of the red fluorescent cells also fluoresce green, highlighting that the population of *phox2bb*<sup>-</sup> neurons is minimal and that *phox2bb* is expressed in nearly all enteric neurons.

Statistical analysis of the total number of *phox2bb*<sup>+</sup> neurons showed no significant difference between wildtype and heterozygous embryos ( $p = 0.1364$ ). However, a significant reduction in GFP<sup>+</sup> neurons was observed in homozygous mutants compared to both wildtype ( $p = 0.0004$ ) and heterozygous embryos ( $p = 0.0209$ ) (Figure 11).

These findings suggest that *mab21l2* is crucial for maintaining the overall population of *phox2bb*<sup>+</sup> neurons. While heterozygous individuals exhibit a slight but non-significant reduction in GFP<sup>+</sup> neuron counts compared to wildtypes, the homozygous mutants show a pronounced decline, underscoring the necessity of *mab21l2* for proper ENS development.

**phox2bb negative neuron percentage are significantly reduced in anti-HuC/D and anti-GFP mab21l2 mutants, suggesting an instructive role for mab21l2 in the specification of phox2bb-neurons in the enteric nervous system**

Percentage of *phox2bb* – neurons of total cells in Anti-GFP and Anti-HuC/D stained 5dpf embryos as seen in wildtypes, heterozygous mutants and homozygous mutants for *mab21l2* at 20x magnification

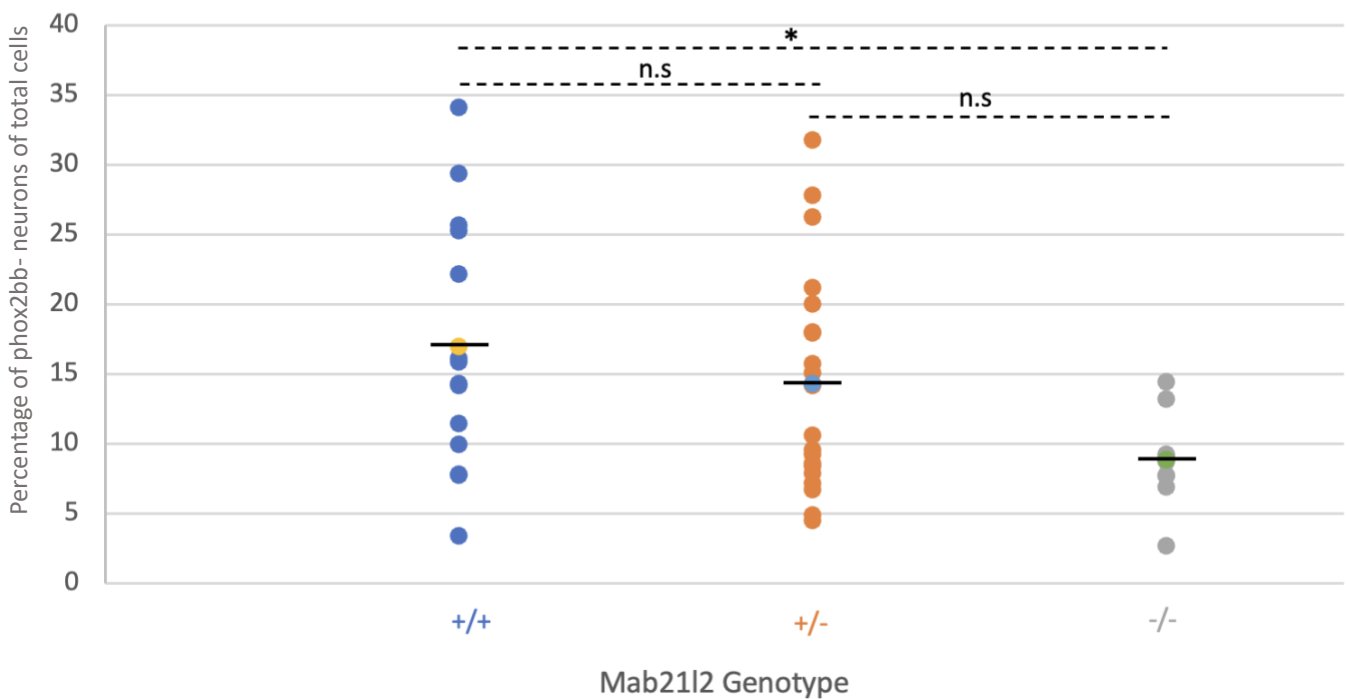


Figure 12: *phox2bb*- neuron percentage at 5dpf across wildtype, heterozygote, and homozygous mutant embryos for the *mab21l2* gene stained with anti-GFP and anti-HuC/D antibodies. No significant difference between the Wildtype and Heterozygote, and between mutant and heterozygote mutant with threshold  $p>0.05$ . *Homozygous* mutants display a significantly lower percentage of *phox2bb*- cells than wildtypes with threshold  $p<0.05$ (denoted by \*)

### Analysis of the Percentage of *phox2bb*- cells as a Proportion of Total Neurons

To evaluate the proportion of *phox2bb*- cells within the enteric neuronal population, we calculated the percentage of red fluorescent (*phox2bb*-) cells relative to the total number of neurons, which are identified as all red fluorescent cells (both *phox2bb*- and *phox2bb*+). In this analysis, *phox2bb*- neurons fluoresce red without any overlapping green fluorescence, while *phox2bb*+ neurons exhibit both red and green fluorescence.

*phox2bb*- cells, on the other hand, include a heterogeneous mix of cells, many of which may not be neurons at all. These could include glial cells, mesenchymal cells, or other cell types within the gut.

Statistical analysis revealed no significant difference in the percentage of *phox2bb*- cells between wildtype and heterozygous embryos ( $p = 0.9359$ ) or between heterozygotes and homozygous mutants ( $p = 0.1548$ ) (Figure 12). However, a significant decrease in the percentage of *phox2bb*- cells was observed in homozygous mutants compared to wildtypes ( $p = 0.04$ ).

These findings highlight that the loss of *mab2112* function in homozygous mutants affects the proportion of these cells, indicating a potential dose-dependent/ instructive role of *mab2112* in maintaining or regulating this population.

## *phox2bb*<sup>+</sup> and nNos<sup>+</sup> Cell Counts

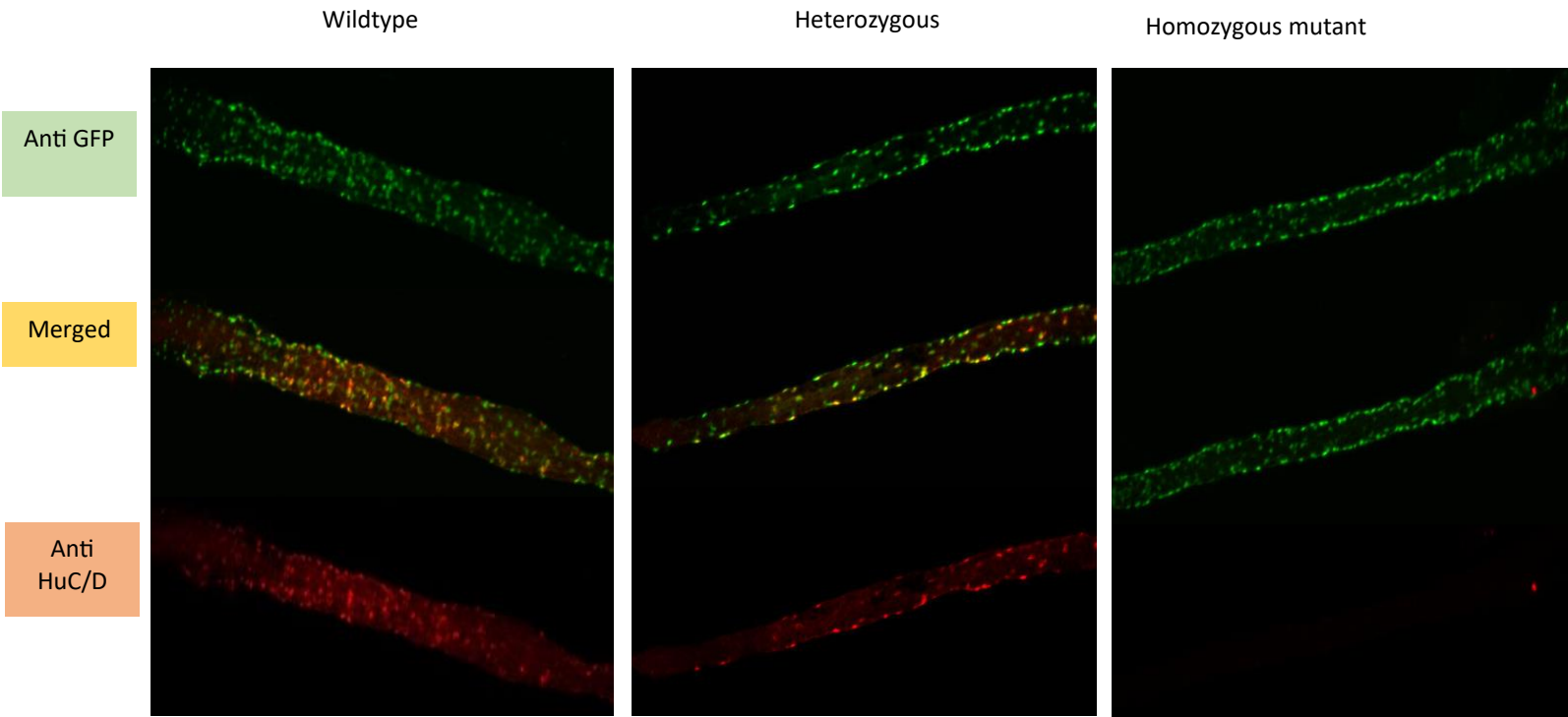


Figure 13: confocal images of wildtype, heterozygous, and homozygous mutant zebrafish guts at 5dpf embryos stained with Anti-GFP and Anti-nNos markers. The guts of *mab21l2* homozygous mutant embryos show a decrease in the number of *phox2bb*<sup>+</sup> cells and a significant loss in percentage of nNos cells.

*phox2bb* positive cells are significantly reduced in anti-GFP and anti-nnos *mab21l2* mutants,  
suggesting an integral role for *mab21l2* in the general development neurons in the enteric  
nervous system.

Number of *phox2bb* + cells in anti-GFP and anti-nNos stained 5dpf embryos as seen in wildtypes, heterozygous mutants and homozygous mutants for *mab21l2* at 10x magnification

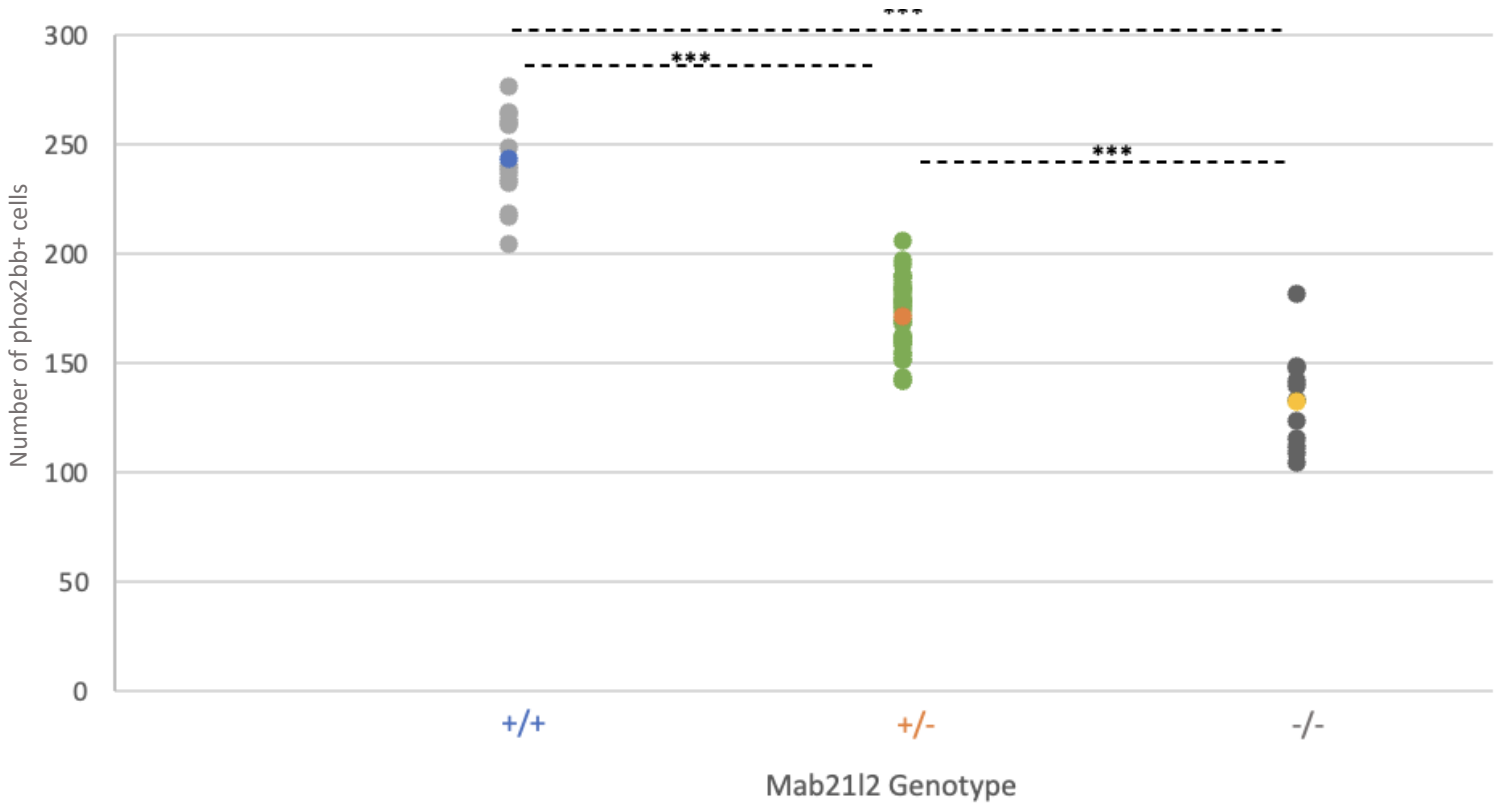


Figure 14: Total number of *phox2bb*+ neurons in 5dpf across wildtype, heterozygote, and homozygous mutant embryos for the *mab21l2* gene stained with anti-GFP and anti-nNos antibodies. Significant differences observed between the total number of neurons between all genotypes with threshold p<0.001 (denoted by \*\*\*).

*mab21l2* homozygous mutant embryos stained with anti-GFP and anti-nNOS antibodies exhibited a significantly lower total number of *phox2bb*<sup>+</sup> enteric cells compared to heterozygous and wildtype embryos at 5 days post-fertilization (5 dpf). To investigate whether the *mab21l2* mutation affects the differentiation of nNOS<sup>+</sup> inhibitory motor neurons, we stained 16 wildtypes, 35 heterozygotes, and 11 homozygous mutants with a combination of anti-GFP and anti-nNOS primary antibodies and complementary secondary antibodies (goat anti-mouse Alexa Fluor 488 and goat anti-rabbit Alexa Fluor 594). Representative gut images for all three genotypes are shown in Figure 14.

In these images, each red dot represents an inhibitory motor neuron expressing the *nos1* gene, which encodes neuronal nitric oxide synthase (nNOS), as detected by the anti-nNOS antibody. Green dots correspond to *phox2bb*<sup>+</sup> enteric cells, which express the *phox2bb* gene and produce GFP, recognized by the anti-GFP antibody. The images reveal that most red fluorescent cells (nNOS<sup>+</sup>) also fluoresce green (*phox2bb*<sup>+</sup>), indicating that the majority of enteric cells producing neuronal nitric oxide synthase are also *phox2bb*<sup>+</sup> enteric neurons.

Comparison of gut images across genotypes indicates a significant decrease in the total number of *phox2bb*<sup>+</sup> cells in heterozygous embryos compared to wildtypes. further, a significant reduction in *phox2bb*<sup>+</sup> cells is also observed in *mab21l2* homozygous mutants relative to both wildtype and heterozygous embryos. Statistical analysis confirms this observation, with the total number of *phox2bb*<sup>+</sup> cells significantly lower in mutants compared to wildtypes ( $p = 7.656 \times 10^{-11}$ ) and heterozygotes ( $p = 1.568 \times 10^{-7}$ ). The difference between wildtypes and heterozygotes is also statistically significant ( $p = 8.504 \times 10^{-5}$ ).

**nNOS positive neuron percentage is significantly reduced in anti-GFP and anti-nNos mab21l2 mutants, suggesting an instructive role for mab21l2 in the specification of inhibitory motor neurons in the enteric nervous system**

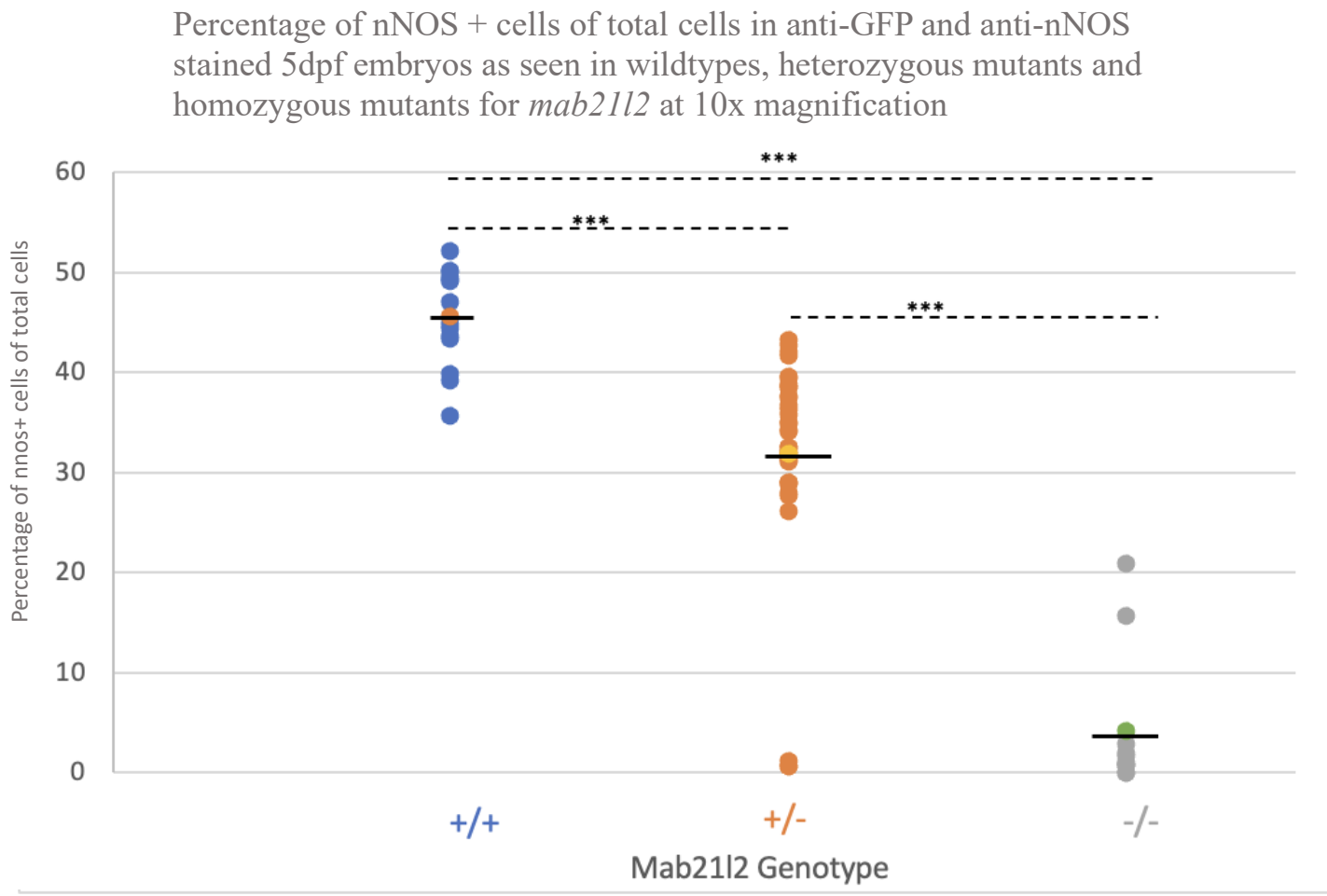


Figure 15: percentage of *phox2bb*+ cells that are nNOS+ in 5dpf across wildtype, heterozygote, and homozygous mutant embryos for the *mab21l2* gene stained with anti-GFP and anti-nNOS antibodies. Significant differences observed between the total number of neurons between all genotypes with threshold  $p < 0.001$  (denoted by \*\*\*).

Subsequently, the percentage of nNOS+ enteric neurons relative to the total count of *phox2bb*+ enteric cells in embryos of the three genotypes was analyzed. Statistical analysis revealed significant differences between all three groups. The percentage of nNOS+ enteric neurons in heterozygotes was significantly lower than in wildtypes ( $p = 1.594 \times 10^{-5}$ ). A further significant reduction in nNOS+ neuron percentages was observed in homozygous mutants compared to both wildtypes ( $p = 2.226 \times 10^{-15}$ ) and heterozygotes ( $p = 3.759 \times 10^{-10}$ ) (Figure 15).

This pronounced reduction in the percentage of nNOS+ neurons in homozygous mutants is consistent with our earlier findings of a severe reduction in the total number of nNOS+ neurons in this genotype. However, the reduction in nNOS+ neurons relative to total *phox2bb*+ cells is greater, suggesting that the loss of nNOS+ neurons is disproportionately higher compared to the loss of the broader *phox2bb*+ enteric cell population. This phenomenon likely reflects a critical role for *mab21l2* in the differentiation or maintenance of nNOS+ inhibitory motor neurons.

When examining the distribution of nNOS+ cells, wildtype and heterozygous embryos exhibit comparable numbers of immunopositive cells, which are evenly distributed across the gut. In contrast, *mab21l2* homozygous mutants show a notable reduction in the total number of nNOS+ cells. Notably, there is a near complete absence of nNOS+ cells in the gut of homozygous mutants. The data demonstrate that *mab21l2* homozygous mutants experience a disproportionate loss of nNOS+ enteric neurons compared to total *phox2bb*+ enteric cells, resulting in a significantly reduced percentage of nNOS+ neurons. These findings underscore the importance of *mab21l2* in regulating specific neuronal subtypes within the ENS.

Although statistical analysis yielded highly significant p-values, it is important to acknowledge the limitations of this dataset due to the relatively low sample size, particularly in the mutant group ( $n = 11$ ). A small sample size can reduce the robustness and reliability of statistical results,

potentially inflating the observed significance. Therefore, while the trends in *phox2bb*+ and nNOS+ cell counts are consistent with the qualitative observations, caution should be exercised when interpreting the results. Future studies with larger sample sizes are needed to confirm these findings and ensure their reproducibility.

## Discussion

This study provides a detailed analysis of the role of *mab21l2* in the development and differentiation of distinct enteric neuronal subtypes in zebrafish. By examining *phox2bb*+, serotonergic (5HT+), *phox2bb*-, and nNOS+ inhibitory motor neurons, we identified specific and broad disruptions in enteric nervous system (ENS) development associated with the loss of *mab21l2*. These findings highlight the gene's critical importance in maintaining neuronal populations and underscore its selective influence on the specification and maintenance of certain specific enteric neuronal subtypes (Furness *et al.*, 2014; Wang *et al.*, 2018).

The significant reduction in *phox2bb*+ enteric cells observed in *mab21l2* homozygous mutants compared to heterozygous and wildtype embryos highlights the essential role of *mab21l2* in regulating the entire enteric neuronal population (Shepherd & Eisen, 2011; Goldstein *et al.*, 2013). *phox2bb*+ cells include nearly all differentiated enteric neurons and undifferentiated neural crest precursors, making this marker a reliable indicator of overall ENS health (Hao & Young, 2009). The loss of *mab21l2* affects both the differentiation and maintenance of these cells, suggesting that it plays a foundational role in the development of the ENS.

Interestingly, while the total number of *phox2bb*+ cells was reduced, there was no evidence of aganglionosis, a phenotype associated with other ENS mutations, such as in *ret* or *phox2b* (Furness *et al.*, 2014; Wang *et al.*, 2018). This observation suggests that *mab21l2* supports

neuronal survival and differentiation rather than affecting enteric neural crest cell (ENCC) migration. Unlike *ret* mutants, which fail to colonize the distal gut due to impaired ENCC migration, *mab21l2* mutants show widespread neuronal losses, indicating a broader regulatory role (Wang *et al.*, 2018).

The disruption in *phox2bb*<sup>+</sup> neuronal populations may reflect impaired transcriptional regulation of survival pathways, as seen with other transcription factors like *sox10*, which drives neuronal differentiation and mitigates apoptosis (Elworthy *et al.*, 2005). Additionally, *mab21l2* may interact with subtype-specific regulators, such as *nkx2-1* or *foxd3*, to ensure that enteric neural crest cells adopt specific neuronal fates (Hendershot *et al.*, 2018; Cooper *et al.*, 2019). This role warrants further investigation through transcriptomic and epigenetic studies.

In contrast to the broad reduction in *phox2bb*<sup>+</sup> cells, the total number of 5HT<sup>+</sup> cells, including serotonergic neurons and non-neuronal enteroendocrine cells, was preserved across genotypes. This finding suggests that serotonergic neurons are less reliant on *mab21l2* for their differentiation or survival. Instead, their development may be governed by alternative transcriptional regulators, such as *pet1*, *lmx1b*, and *gata2*, which are known to regulate serotonin synthesis and neuronal differentiation in vertebrate models (Gaspar *et al.*, 2003;). The non-significant reduction in 5-HT-positive neurons observed in mutants corresponds well with diminished clustering of *tph1b*, further supporting the idea of a less direct role for *mab21l2* in promoting serotonergic differentiation. However, the altered proportion of nNOS<sup>+</sup> neurons in mutants indicates that *mab21l2* may still indirectly influence this population, potentially by modulating upstream pathways or transcriptional programs shared between subtypes. The preservation of serotonergic neurons may also reflect compensatory mechanisms that prioritize this critical neuronal subtype. Serotonergic neurons play an essential role in regulating

gut motility and sensory reflexes, functions that are vital for gastrointestinal homeostasis (Gershon, 2013). Their stability in *mab21l2* mutants may suggest evolutionary pressure to safeguard this population against developmental disruptions. This hypothesis aligns with findings in other ENS models, such as *ednrb* and *sox10* mutants, where serotonergic neurons were less affected than other subtypes despite broader disruptions in ENS development (Lake & Heuckeroth, 2013).

Additionally, serotonergic neurons are among the earliest neuronal subtypes to differentiate during ENS development, which may render them less susceptible to disruptions occurring later in the developmental timeline (Hao & Young, 2009). The relative stability of serotonergic neuron proportions across genotypes, despite the reduction in *phox2bb*+ cells, underscores the robustness of this population and suggests that it is regulated by distinct transcriptional and signaling pathways.

The HuC/D staining data revealed a decreased proportion of *phox2bb*- neurons in *mab21l2* homozygous mutants, along with the overall reduction in HuC/D+ neurons. *phox2bb*- neurons, identified by their red fluorescence without overlapping GFP fluorescence, represent a small population of enteric neurons that do not express the *phox2bb* gene. This suggests that *mab21l2* specifically regulates the differentiation or survival of *phox2bb*+ lineages, as well as *phox2bb*- populations (Elworthy et al., 2005; Cooper et al., 2019). The overlap in of *mab21l2* and *elavl3* in UMAP expression occurs within specific clusters suggests that *mab21l2* is expressed in cells that are transitioning into mature neuronal states. This observation aligns with the reduction in total enteric neuron numbers in mutants, emphasizing that *mab21l2* may be broadly required for the differentiation and survival of enteric neurons. The observed decrease in the proportion of *phox2bb*- neurons in mutants, coupled with the UMAP clustering patterns, suggests that *mab21l2*

is not only involved in the generation of *phox2bb*<sup>+</sup> neurons but also in maintaining balanced neuronal subtype proportions.

The decrease in the percentage of *phox2bb*<sup>-</sup> neurons in mutants likely reflects a selective loss of this population rather than a simple failure of ENCC progenitors to differentiate into *phox2bb*<sup>+</sup> neurons. This disproportionate reduction suggests that *phox2bb*<sup>-</sup> neurons may rely more critically on *mab21l2* for their maintenance or survival compared to *phox2bb*<sup>+</sup> neurons (Burns *et al.*, 2020). Unlike findings with other ENS regulators, such as *sox10*, where impaired neuronal differentiation alters subtype proportions without reducing overall cell numbers (Elworthy *et al.*, 2005), the observed decrease in *phox2bb*<sup>-</sup> neurons highlights a unique dependence on *mab21l2*, potentially due to its role in stabilizing or supporting this developmentally distinct population. Among all neuronal subtypes examined, nNOS<sup>+</sup> inhibitory motor neurons were the most severely affected by the loss of *mab21l2*. Homozygous mutants exhibited significant reductions in both the total number and percentage of nNOS<sup>+</sup> neurons relative to *phox2bb*<sup>+</sup> cells. Furthermore, the spatial distribution of nNOS<sup>+</sup> neurons was disrupted, with most cells concentrated in the anterior gut and a marked absence in distal regions.

The disproportionate loss of nNOS<sup>+</sup> neurons highlights the importance of *mab21l2* in the differentiation and maintenance of this neuronal subtype. Studies in mammals have shown that inhibitory motor neurons depend on transcription factors such as *nkx2-1*, *foxd3*, and *phox2b* for their specification and function. The disruption of nNOS<sup>+</sup> neurons in *mab21l2* mutants suggests that *mab21l2* operates within a similar regulatory network, potentially upstream or in conjunction with these factors.

Unlike serotonergic neurons, which may be preserved through compensatory mechanisms, nNOS<sup>+</sup> neurons appear more vulnerable to disruptions in transcriptional regulation. This

vulnerability may reflect their later differentiation during ENS development, as later-maturing subtypes are often more susceptible to disruptions in regulatory pathways (Hao & Young, 2009). The absence of distal nNOS+ neurons in *mab21l2* mutants further underscores the gene's role in establishing proper neuronal distribution along the gut.

The differential effects of *mab21l2* loss on *phox2bb*+ cells, serotonergic, *phox2bb*-, and nNOS+ neurons highlight the complexity of ENS development and the distinct molecular pathways that govern neuronal differentiation. While serotonergic populations are relatively preserved, nNOS+ neurons, *phox2bb*- neurons, and the broader *phox2bb*+ cell population are significantly disrupted, suggesting that *mab21l2* serves as both a general regulator and a subtype-specific factor within the ENS.

### Conclusions

This study demonstrates the critical role of *mab21l2* in regulating ENS development in zebrafish. The loss of *mab21l2* results in significant reductions in the total population of *phox2bb*+ cells, with a disproportionate impact on *phox2bb*- neurons and nNOS+ inhibitory motor neurons, while serotonergic neurons are only proportionately affected.

## Bibliography

1. **A. S., & Burns, A. J.** (2005). Development of the enteric nervous system, smooth muscle and interstitial cells of Cajal in the human gastrointestinal tract. *Cell and Tissue Research*, 319(3), 367–382. <https://doi.org/10.1007/s00441-004-1023-2>
2. **Amiel, J., Sproat-Emison, E., Garcia-Barcelo, M., Lantieri, F., Burzynski, G., Borrego, S., Pelet, A., Arnold, S., Miao, X., Griseri, P., Brooks, A. S., Antinolo, G., de Pontual, L., Clement-Ziza, M., Munnich, A., Kashuk, C., West, K., Wong, K. K. Y., Lyonnet, S., Chakravarti, A., ... & Hirschsprung Disease Consortium.** (2008). Hirschsprung disease, associated syndromes and genetics: A review. *Journal of Medical Genetics*, 45(1), 1–14. <https://doi.org/10.1136/jmg.2007.053959>
3. **Bellono, N. W., Bayrer, J. R., & Julius, D.** (2017). Enterochromaffin cells are gut chemosensors that couple to sensory neural pathways. *Cell*, 170(1), 185–198.e16. [10.1016/j.cell.2017.05.034](https://doi.org/10.1016/j.cell.2017.05.034)
4. **Boesmans, W., Hao, M. M., & Vanden Berghe, P.** (2015). Imaging neuron-glia interactions in the enteric nervous system. *Frontiers in Cellular Neuroscience*, 9, 379. <https://doi.org/10.3389/fncel.2013.00183>
5. **Brookes, S. J. H.** (2001). Classes of enteric nerve cells in the guinea-pig small intestine. *Anatomy and Embryology*, 204(1), 3–10. [https://doi.org/10.1002/1097-0185\(20010101\)262:1<58::AID-AR1011>3.0.CO;2-V](https://doi.org/10.1002/1097-0185(20010101)262:1<58::AID-AR1011>3.0.CO;2-V)
6. **Burns, A. J., & Pachnis, V.** (2009). Development of the enteric nervous system: Bringing together cells, signals, and genes. *Neurogastroenterology & Motility*, 21(2), 100–102. <https://doi.org/10.1111/j.1365-2982.2008.01255.x>

7. **Burns, A. J., & Thapar, N.** (2006). Neural stem cell therapies for enteric nervous system disorders. *Nature Clinical Practice Gastroenterology & Hepatology*, 3(11), 531–541. <https://doi.org/10.1038/nrgastro.2013.226>
8. **Butler Tjaden, N. E., & Trainor, P. A.** (2013). The developmental etiology and pathogenesis of Hirschsprung disease. *Translational Research*, 162(1), 1–15. <https://doi.org/10.1016/j.trsl.2013.03.001>
9. **Cooper, J. E., McCann, C. J., & Trainor, P. A. (2016).** Sox10 and endothelin 3 cooperatively control the timing of enteric neurogenesis. *Developmental Biology*, 411(2), 352–360. <https://doi.org/10.1016/j.ydbio.2016.01.017>
10. **Costa, M., Brookes, S. J. H., & Hennig, G. W.** (2000). Anatomy and physiology of the enteric nervous system. *Gut*, 47(Suppl 4), iv15–iv19. [https://doi.org/10.1136/gut.47.suppl\\_4.iv15](https://doi.org/10.1136/gut.47.suppl_4.iv15)
11. **Furness, J. B.** (2006). *The Enteric Nervous System*. Blackwell Publishing. <https://doi.org/10.1002/9780470988756>
12. **Furness, J. B.** (2012). The enteric nervous system and neurogastroenterology. *Nature Reviews Gastroenterology & Hepatology*, 9(5), 286–294. <https://doi.org/10.1038/nrgastro.2012.32>
13. Furness, J. B., Callaghan, B. P., Rivera, L. R., & Cho, H.-J. (2014). The enteric nervous system and gastrointestinal innervation: Integrated local and central control. *Advances in Experimental Medicine and Biology*, 817, 39–71. [https://doi.org/10.1007/978-1-4939-0897-4\\_3](https://doi.org/10.1007/978-1-4939-0897-4_3)

14. **Gaspar, P., Cases, O., & Maroteaux, L. (2003).** The developmental role of serotonin: News from mouse molecular genetics. *Nature Reviews Neuroscience*, 4(12), 1002–1012. <https://doi.org/10.1038/nrn1256>

15. **Gershon, M. D., & Tack, J. (2007).** The serotonin signaling system: From basic understanding to drug development for functional GI disorders. *Gastroenterology*, 132(1), 397–414. <https://doi.org/10.1053/j.gastro.2006.11.002>

16. **Grundy, D. (2006).** Signalling the state of the digestive tract. *Autonomic Neuroscience Volume 125, Issues 1–2* 1682–1693.  
<https://doi.org/10.1136/gut.2005.091850>

17. **Hao, M. M., Bornstein, J. C., & Young, H. M. (2016).** Development of myenteric cholinergic neurons in ChAT–eGFP transgenic mice. *The Journal of Comparative Neurology*, 524(14), 2645–2661. <https://doi.org/10.1002/cne.23354>

18. **Heanue, T. A., & Pachnis, V. (2007).** Enteric nervous system development and Hirschsprung’s disease: Advances in genetic and stem cell studies. *Nature Reviews Neuroscience*, 8(6), 466–479. <https://doi.org/10.1038/nrn2137>

19. **Kuil, L. E., Chauhan, R. K., Cheng, W. W., Hofstra, R. M. W., & Alves, M. M. (2020).** Zebrafish: A model organism for studying enteric nervous system development and disease. *Frontiers in Cell and Developmental Biology*, 8, 629073.  
<https://doi.org/10.3389/fcell.2020.629073>

20. **Kunze, W. A. A., & Furness, J. B. (1999).** The enteric nervous system and regulation of intestinal motility. *Annual Review of Physiology*, 61, 117–142.  
<https://doi.org/10.1146/annurev.physiol.61.1.117>

21. **Lake, J. I., & Heuckeroth, R. O.** (2013). Enteric nervous system development: Migration, differentiation, and disease. *American Journal of Physiology-Gastrointestinal and Liver Physiology*, 305(1), G1–G24.  
<https://doi.org/10.1152/ajpgi.00452.2012>

22. **Lake, J. I., & Heuckeroth, R. O. (2013). Enteric nervous system development: Migration, differentiation, and disease. *American Journal of Physiology-Gastrointestinal and Liver Physiology*, 305(1), G1–G24.**  
<https://doi.org/10.1152/ajpgi.00452.2012>

23. **Lasrado, R., Boesmans, W., Kleinjung, T., Pin, C., Bell, D., Bhaw, L., McCallum, S., Zong, H., Luo, L., Clevers, H., Pachnis, V., & Vanden Berghe, P.** (2017). Lineage-dependent spatial and functional organization of the mammalian enteric nervous system. *Science*, 356(6339), 722–726. [DOI: 10.1126/science.aam7511](https://doi.org/10.1126/science.aam7511)

24. **Nagy, N., & Goldstein, A. M.** (2017). Enteric nervous system development: A crest cell's journey from neural tube to colon. *Seminars in Cell & Developmental Biology*, 66, 94–106. <https://doi.org/10.1016/j.semcd.2017.01.006>

25. **Nezami, B. G., & Srinivasan, S.** (2010). Enteric nervous system in the small intestine: Pathophysiology and clinical implications. *Current Gastroenterology Reports*, 12(5), 358–365. <https://doi.org/10.1007/s11894-010-0129-9>

26. **Nurgali, K., Nguyen, T. V., Matsuyama, H., Thacker, M., Robbins, H. L., & Furness, J. B. (2007).** Phenotypic changes of morphologically identified guinea-pig myenteric neurons following intestinal inflammation. *The Journal of Physiology*, 583(2), 593–609. <https://doi.org/10.1113/jphysiol.2007.135947>

27. **Olsson, C., & Holmgren, S.** (2001). The control of gut motility. *Comparative Biochemistry and Physiology Part A: Molecular & Integrative Physiology*, 128(3), 481–503. [https://doi.org/10.1016/S1095-6433\(00\)00330-5](https://doi.org/10.1016/S1095-6433(00)00330-5)

28. **OpenStax College.** (2013). *Anatomy & Physiology*. OpenStax CNX. Retrieved from <https://openstax.org/books/anatomy-and-physiology/pages/1-introduction>

29. **Rao, M., & Gershon, M. D.** (2016). Enteric nervous system development and Hirschsprung's disease: Advances in genetic and stem cell studies. *Developmental Biology*, 417(2), 209–219. <https://doi.org/10.1016/j.ydbio.2016.04.006>

30. **Rao, M., & Gershon, M. D. (2016). The bowel and beyond: The enteric nervous system in neurological disorders. *Nature Reviews Gastroenterology & Hepatology*, 13(9), 517–528.** <https://doi.org/10.1038/nrgastro.2016.107>

31. **Sang, Q., & Young, H. M.** (1998). The identification and chemical coding of cholinergic neurons in the small and large intestine of the mouse. *Anatomy and Embryology*, 194(5), 475–490. [https://doi.org/10.1002/\(SICI\)1097-0185\(199806\)251:2<185::AID-AR6>3.0.CO;2-Y](https://doi.org/10.1002/(SICI)1097-0185(199806)251:2<185::AID-AR6>3.0.CO;2-Y)

32. **Shepherd, I. T., & Eisen, J. S.** (2011). Development of the zebrafish enteric nervous system. *Methods in Cell Biology*, 101, 143–160. <https://doi.org/10.1016/B978-0-12-387036-0.00006-2>

33. **Wood, J. D.** (2008). Enteric nervous system: Reflexes, pattern generators and motility. *Current Opinion in Gastroenterology*, 24(2), 149–158. <https://doi.org/10.1097/MOG.0b013e3282f56125>

34. **Zeisel, A., Hochgerner, H., Lönnerberg, P., Johnsson, A., Memic, F., Van Der Zwan, J., Häring, M., Braun, E., Borm, L. E., La Manno, G., Codeluppi, S.**

**Furlan, A., Lee, K., Skene, N., Harris, K. D., Hjerling-Leffler, J., Arenas, E., Ernfors, P., Marklund, U., & Linnarsson, S.** (2018). Molecular architecture of the mouse nervous system. *Cell*, 174(4), 999–1014.

<https://doi.org/10.1016/j.cell.2018.06.021>